Zhu *et al.*
Chinese Journal of Mechanical Engineering (2022) 35:148
https://doi.org/10.1186/s10033-022-00818-w

Chinese Journal of Mechanical Engineering

REVIEW

Open Access

Recent Advances in Drilling Tool Temperature: A State-of-the-Art Review

Zhaoju Zhu[1*], Xinhui Sun[1], Kai Guo[2], Jie Sun[2] and Jianfeng Li[2]

Abstract

Drilling is regarded as the most complex manufacturing process compared with other conventional machining processes. During the drilling process, most of the energy consumed in metal cutting is converted to heat and increases temperature considerably. The resulting thermal phenomena are important since they influence the mode of deformation, the final metallurgical state of the machined surface, and the rate of tool wear. Hence, understanding the temperature characteristics in the drilling process is crucial for enhancing the drill performance and process efficiency. Extensive efforts have been conducted to measure and control the drilling tool temperature successively. However, very few studies have been conducted from a comprehensive perspective to review all the efforts. To address this gap in the literature, a rigorous review concerning the state-of-the-art results and advances in drilling tool temperature is presented in this paper by referring to the wide comparisons among literature analyses. The multiple aspects of drilling tool temperature are precisely detailed and discussed in terms of theoretical analysis and thermal modeling, methods for temperature measuring, the effect of cutting parameters, tool geometries and hole-making methods on temperature and temperature controlling by different cooling methods. In conclusion, several possible future research directions are discussed to offer potential insights for the drilling community and future researchers.

Keywords: Drilling, Tool temperature, Advance materials, Cutting characteristics

1 Introduction

With the rapid development of the aerospace industry, the application of advanced materials such as titanium alloys, carbon fiber reinforced polymer (CFRP), or hybrid CFRP/Ti stacks is widely increasing. For these advanced materials, there are various disadvantages in the machining process due to their inherent properties, which can easily result in excessive cutting force, high cutting temperatures, severe tool wear and poor surface quality. All these present a serious challenge to mechanical processing. As one of the most common and necessary processing technologies, drilling is taking widely used in automotive, aerospace and many other industries to produce holes of various sizes and depths. In addition, it is usually one of the final steps in the fabrication of mechanical components and has considerable economical importance. For example, in order to meet the process conditions such as component connection and assembly, mechanical components generally need to be subjected to secondary machining after forming, and drilling accounts for 50% of the secondary machining [1]. According to statistics, there are about 3 million assembly holes in an aircraft, and the cost of the holes accounts for about 3%-5% of the entire aircraft [2, 3]. In the working process of the aircraft, due to the influence of cyclic stress, the assembly holes are prone to generate fatigue damage, and more than 30% of the aircraft failures are caused by the quality of the holes [4]. Therefore, it is of great significance to achieve high-efficiency and high-quality drilling processing.

As a semi-closed processing method, drilling is also regarded as the most complex manufacturing process compared with other conventional machining processes

*Correspondence: zhuzhaoju0216@163.com

[1] School of Mechanical Engineering and Automation, Fuzhou University, Fuzhou 350116, China
Full list of author information is available at the end of the article

(turning, milling, boring, etc). During the drilling process, most of the mechanical energy required for the metal cutting process is converted into heat which is transferred into the chip, the workpiece and the cutting tool. So drilling can achieve higher temperatures than other processing methods. Related research has shown that drilling temperature plays a significant role in drilling performance and tool wear [5]. This is owing to the fact that the special working environment of drilling makes it difficult for chips to evacuate, which leads to a large amount of heat accumulating, rapid tool wear and greatly shortens the service life of the tool. Furthermore, due to the increase of the drilling temperature, it may cause material softening and thus affect the tool life and hole-making quality. Therefore, strengthening the research on drilling temperature and further understanding the mechanism of the interaction between temperature and various parameters in the drilling process are extremely important for extending tool life, reducing the surface roughness of the hole, improving the quality of the hole, and improving the performance of the workpiece [6]. In recent years, extensive efforts have been conducted to measure and control the tool temperature in material removal processes, including temperature measuring methods, the effect of processing parameters and tool geometries, and different hole-making processes, etc. However, to the best of the authors' knowledge, very few studies have been conducted from a comprehensive perspective. An up-to-date, critical review of the drilling tool temperature is necessary.

For this purpose, the authors aim to fulfil this requirement and provide a critical overview of the broad field of drilling tool temperature as well as the future works based on the systematic arrangement and analysis of related research. This article is organized into six sections follows by conclusions and outlooks. Its overall structure is illustrated in Figure 1. It begins with the theoretical analysis and modeling of drilling temperature in Section 2. Section 3 outlines the up-to-date development of methods for measuring drilling temperature and describes their measuring principles. Then it elaborates on the effect of cutting parameters, tool geometries and hole-making methods on the drilling temperature in Sections 4, 5, 6, respectively. Furthermore, a variety of auxiliary cooling methods to control the drilling temperature is summarized in Section 7. Finally, the conclusions and possible future research directions for drilling tool temperature are drawn and discussed in Section 8.

2 Theoretical Analysis and Modeling of Drilling Temperature

Cutting heat is an important physical phenomenon in the drilling process, and the drilling temperature is an extremely important factor that affects the performance of the tool and workpiece, such as the hole accuracy, surface roughness and tool wear. Therefore, theoretical analysis on drilling temperature is indispensable, which can help researchers to reduce the tool temperature from the source.

Agapiou et al. regarded the drill as a semi-infinite body to establish an analysis model of the temperature distribution along the cutting edge, and used transient analysis to partition heat among the tool, chips and workpieces to obtain the drilling temperature [7]. Watson et al. proposed a hypothesis that the cutting edge of the drill was regarded as a series of elementary cutting tools, and each elementary cutting tool (ECT) was performed a simple metal cutting operation during the drilling process [8]. Ke et al. calculated the cutting force of each ECT using the thrust and torque measured during drilling, and estimated the chip speed through the chip thickness and shear angle corresponding to each ECT. So the friction and heat generated during the drilling process can be determined [9]. With the development of computer technology, the finite element method has been widely used in mechanical processing. Bono et al. established a model to predict the heat flow into the workpiece, and used embedded thermocouples to conduct experiments to verify that the model can accurately predict the temperature of the workpiece within a certain drilling speed and feed range [10–12]. Fuh et al. also used the finite element method to study the effects of the penetration depth, the web thickness, the cutting speed and the helix angle on drilling temperature and predicted the temperature distribution along the cutting edge [13]. Kalidas et al. established a model to predict the temperature of the workpiece which used the inverse heat transfer method to determine the heat flow and the distribution coefficient of the cutting edge and the chisel edge, and obtained the temperature of the workpiece during the drilling process in both wet and dry conditions with coated and uncoated drills [14, 15]. Kuzu et al. also employed the method of inverse heat conduction and considered the heat convection coefficient after using minimum quantity lubrication (MQL). The inverse method was consistent with the experimental temperature measurement results [16]. Wu et al. proposed a finite element model to predict the drilling temperature based on an equivalent model, which took into account the influence of feed rate on the working rake angle and working relief angle. Results showed that drilling temperature of simulations had good agreement

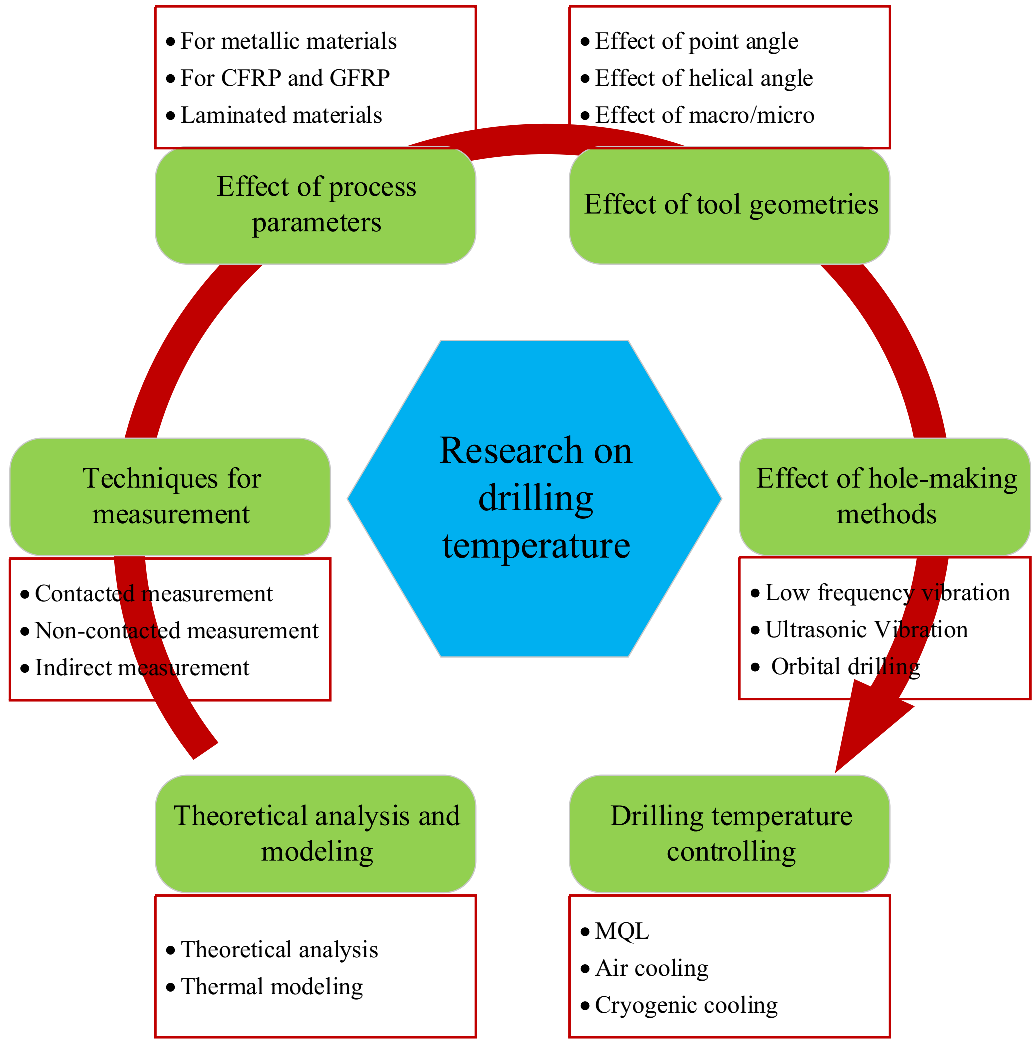

Figure 1 The flow and structure of this paper

with the experimental ones [17]. Camille et al. presented a mixed numerical-experimental approach which relied on the strain and temperature measurements at arbitrary point in the cutting edge of the drill, and then used the measurement results to predict the energy in the material removal process. The results proved that the method can determine the heat generated during the drilling process and the way of heat transfer in the workpiece. The model is shown in Figure 2 [18].

When establishing the temperature model, considering the difference of the workpiece material, the model may be different. Nouari et al. believed that drilling temperature is the most important factor causing tool wear, and utilized experiments and finite element modeling to determine the relationship between tool wear and temperature during aluminum alloy drilling [6]. Because of the anisotropy and heterogeneity of carbon fiber epoxy composites, Zhu et al. established the temperature file model of the unidirectional composites after homogenizing, then conducted experiments with k-type thermocouples and infrared thermometer to measure the drilling temperature at the exit of the hole, and the results showed that the temperature file model was consistent with the experiments [19]. Wang et al. also proposed a fiber orientation-based analytical model to predict the heat partition ratio based on classical hertz contact theory, and the temperature distribution on the workpiece obtained by the infrared thermometer verified the correctness of the model. Furthermore, the fiber orientations had a notable impact on this ratio [20]. Patne et al. developed a comprehensive finite model which considered a variable heat partition and ploughing forces

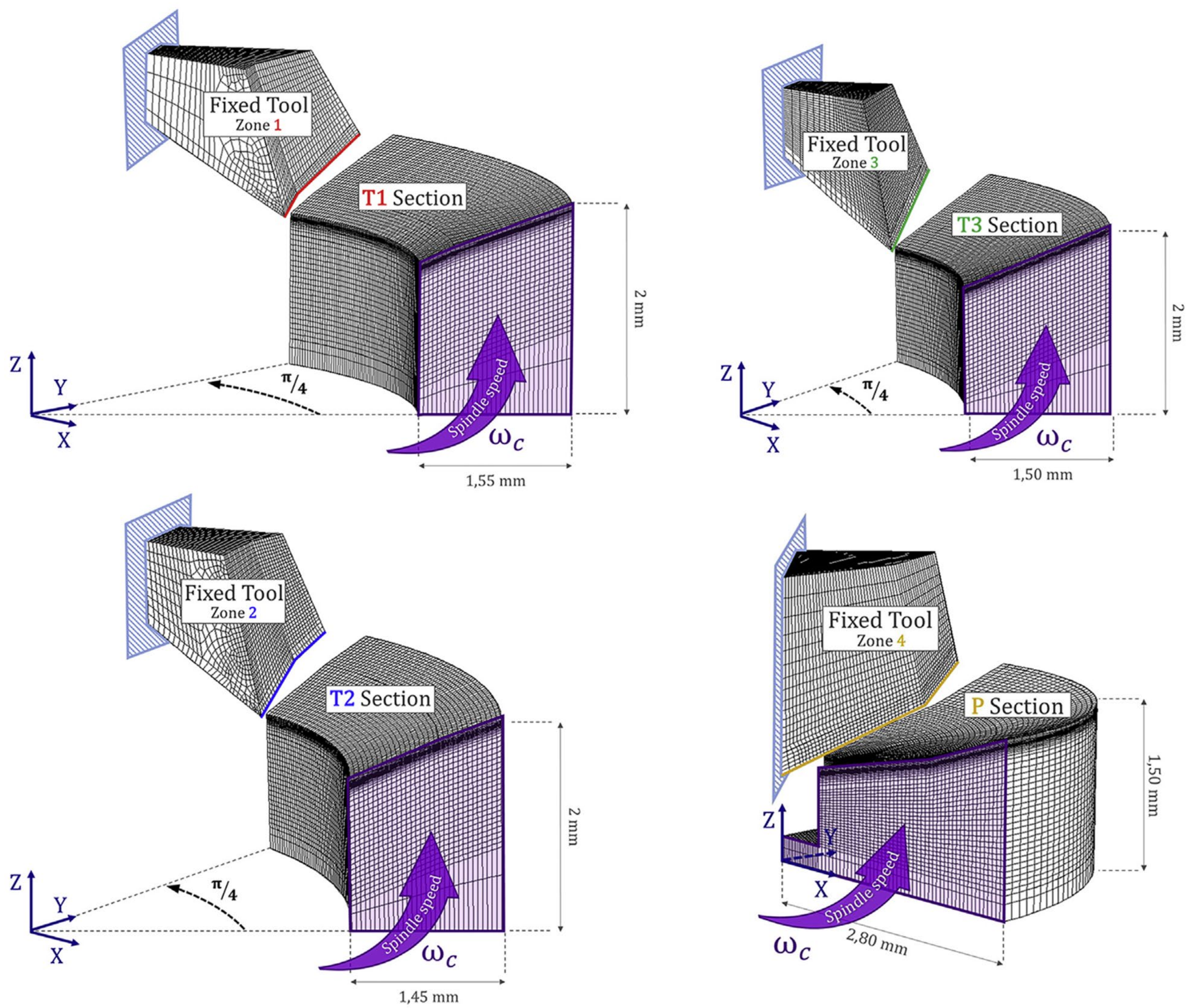

Figure 2 A multi-scale and coupled cutting model for the drilling of Ti6Al4V [18]

for simultaneously estimating the temperature distribution of the tool and the finite element model is shown in Figure 3 [21, 22]. Álvarez et al. considered the thermal phenomena involved in the drilling of composite, and proposed a comprehensive thermal analysis approach, which used both an analytical estimation of heat generated during drilling and numerical modeling for heat propagation and the risk of thermal damage can be obtained indirectly through the measurement of thrust and torque [23].

Most of the models described above divided the drill into ECT (see Table 1) which relied on experimental data such as cutting force, chip thickness and shear angle to measure the temperature. Therefore, obtaining the heat partition ratio is relatively limited. In order to correctly express the heat distribution mechanism among tools, workpieces and chips in the drilling process, it is necessary to further study the theoretical model of cutting heat from the perspective of thermal-mechanical coupling so that researchers can conduct more in-depth research on the drilling temperature.

3 Techniques for Drilling Temperature Measurement

The temperature generated during the drilling process will cause tool wear and shorten tool life. What's more, drilling temperature has a non-negligible effect on the hole quality and surface integrity. Therefore, researchers

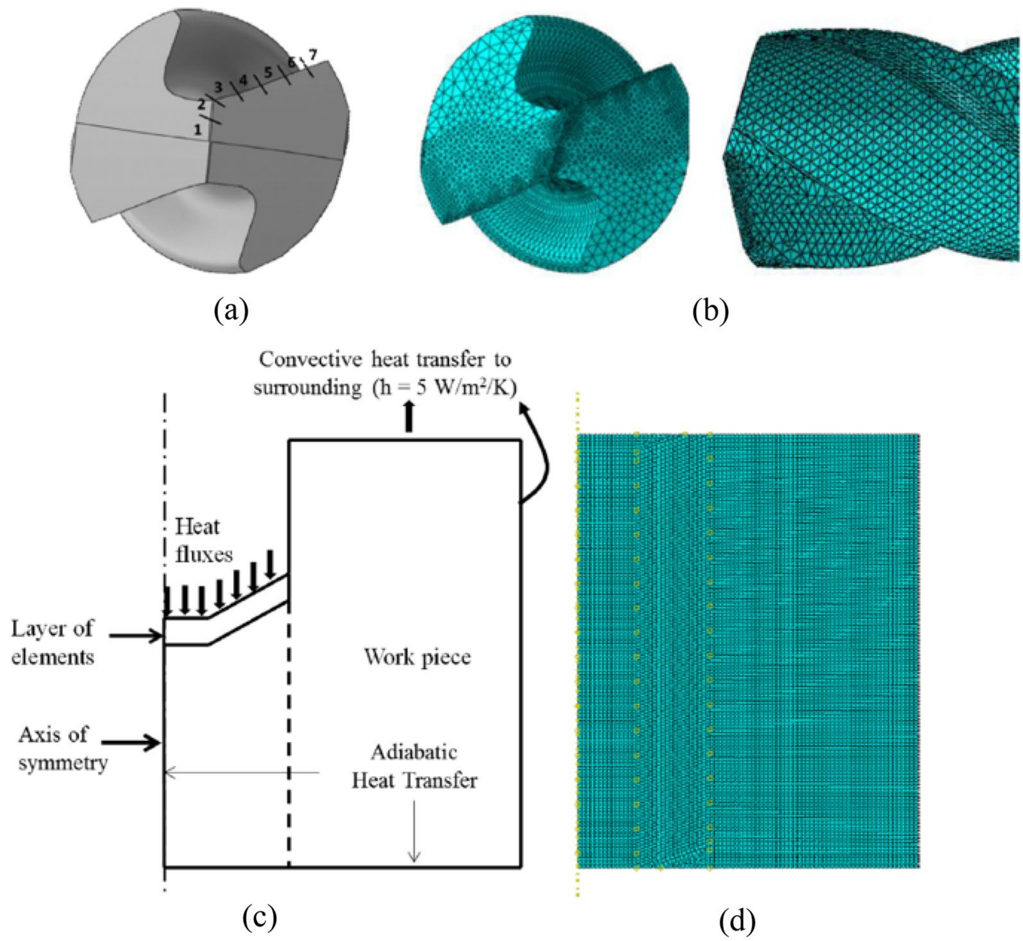

Figure 3 Finite element modeling of workpiece and drill: **a** Location of ECTs on the tool, **b** Mesh for 3D FE thermal model, **c** Schematic of the workpiece for numerical simulations, **d** FE meshing of the workpiece [21]

used various techniques to measure the temperature distribution of the workpiece and tool to minimize the damage caused by the cutting heat, as shown in Figure 4.

As early as the 1940s, Schmidt et al. embedded a thermometer in the workpiece in advance to measure the temperature of the tool, chips and workpiece to determine partition ratio of the cutting heat during the drilling process, then summarized that the heat transferred to the chip accounts for 70%-80%, about 10% in the workpiece and the remaining heat was transferred to the tool [24]. With the development of technology, the existing temperature measurement techniques can be divided into contact measurement, non-contact measurement and indirect measurement. The contact measurement has a long time and a wide range of application among the measurement techniques, mainly include tool-work thermocouple, embedded thermocouple method and tool-foil thermocouple system, which is the most mature method for temperature measurement. However, due to the need to install thermocouples and collect signals when applying contact measurement, there may be problems such as limited installation of thermocouples and difficulty in signal extraction in some cases. Non-contact measurement includes pyrometer, infrared radiation camera, and optical fiber two-color pyrometer, which can measure the drilling temperature simply and intuitively. However, it needs to be calibrated before measurement, and unless specially positioned, it is difficult to measure the temperature when the drill is inside the workpiece. The indirect measurement includes metallographic method and scanning electron microscopy method [25–27], which observes the metallographic changes of metal materials in different high-temperature environments. However, this technique is only applicable to the high temperature above 600℃, and the tool should be destroyed for sample preparation, which makes this technique unable to be popularized.

Table 1 Heat flux models in drilling

Authors and year	Model	Divide into ECTs	Inverse heat conduction	Plowing effect	The materials' property
Agapiou et al. 1994 [7]	$\begin{cases} T_{int}(r_i) = \Delta T_S(r_i) + \Delta T_f(r_i) + T_R \\ \Delta T_S(r_i) = (R_1 \cdot \tau(r_i) \cdot A_S V_s)/(\rho_\omega C_\omega A \cdot V) \\ \Delta T_f(r_i) = 4(1 - R_{2S}(r_i)) \cdot q_{fi}.L_2(r_i)/3 \end{cases}$	YES	NO	NO	NO
Kalidas et al. 2002[14]	$\begin{cases} q_1 = \varnothing_1 \left(\frac{L-Z}{L-d_Z}\right) \\ q_2 = \varnothing_2 \frac{T_{lips}\omega + F_{lips} V_f}{A_{lips}} \\ q_3 = \varnothing_3 \frac{T_{point}\omega + F_{point} V_f}{A_{point}} \end{cases}$	YES	YES	NO	NO
Wu et al. 2009[17]	$\begin{cases} q_{t-c} = q_k + q_r - f_1 q_g \\ q_{t-w} = -q_k - q_r - f_2 q_g \\ q_g = \eta\tau \frac{\Delta S}{\Delta t} \end{cases}$	YES	NO	NO	NO
Bono et al. 2002[9]	$\begin{cases} q''_{wp} = \frac{(1-q_f/q)(T\omega + F_z V_f)}{\pi\left(r_{outer}^2 - r_{inner}^2\right)} \\ q''_{drill} = \frac{(1-R_2)(q_f/q)(T\omega + F_z V_f)}{area\ of\ element} \end{cases}$	YES	NO	NO	NO
Zhu et al. 2012[19]	$q_0 = \frac{\alpha(T\omega + F_z V_f)}{\pi(d/2)^2/\sin 59°}$	YES	NO	NO	YES
Patne et al. 2017[21]	$\begin{cases} q_{tool}^{shear} = (1 - B_d)V_C.\rho_\omega.C_\omega.T_s.b.t_2 \\ q_{tool}^{rake} = (1 - B_k)q_f = (1 - B_k)F_f.V_c \\ q_{tool}^{flank} = (1 - B_f)q_{flank} = (1 - B_f)F_{c\omega}.V \end{cases}$	YES	NO	YES	NO
Álvarez et al. 2014[23]	$\begin{cases} dQ = dW_T + dW_F - dE_f \\ dE_f(\theta) = \omega_f dV_f(\theta) \\ dV_f(\theta) = \pi L_{cut}^2 f_{cut} \frac{d\theta}{2\pi} \end{cases}$	NO	NO	NO	YES
Li et al. 2007[37]	$\begin{cases} Q_{tool}^{friction} = B_2 Q_f = B_2 F_f V_c \\ q''_{tool} = \frac{B_2 q_f}{l_c l} \\ B_2 = (1 + 0.45 \frac{K_t}{K_w} \sqrt{\frac{\pi\alpha_\omega}{V_c l_c}})^{-1} \end{cases}$	YES	YES	NO	NO

3.1 Contact Measurement Techniques

3.1.1 Tool-Work Thermocouple

The tool-work thermocouple is the most common type of thermocouple in machining research, mainly because it's easiest to implement [28, 29]. As seen in Figure 5, the tool-work thermocouple, made up of a tool and a workpiece of different materials, develops an electric motive force when starting drilling. Then the relationship between temperature and electromotive force is found.

Despite its low cost and easy implementation, it is not clear whether the tool-work thermocouple actually measures the average temperature or the lowest temperature. In fact, the electromotive force generated by the tool-work thermocouple does not even match the average temperature of the interface, unless the temperature is uniform or the signal changes linearly with temperature [30, 31]. Therefore, using this kind of thermocouple for measuring temperature is not recommended.

3.1.2 Embedded Thermocouple

The embedded thermocouple is to embed the thermocouple in the workpiece or the tool, and fix it by welding or epoxy resin. Additionally, measuring drilling temperature with embedded thermocouples requires fixing the drill and rotating the workpiece as shown in Figures 6 and 7. Compared with tool-work thermocouples, embedded thermocouples provide higher measurement accuracy, respond faster, and measure a wider temperature range [32–34].

Devries et al. embedded iron-constantan thermocouples at different points on the flank face of the tool to measure the drilling temperature, and they also found that the workpiece properties, such as the presence of pilot holes and the size, affected the drilling temperature substantially [35]. Battaglia et al. inserted the thermocouple into the oil hole of a carbide double cutting drill to determine temperature distribution and estimated the heat fluxes on the cutting edge [36]. Li et al. embedded thermocouple into carved groove on a fixed drill that was continuously sprayed with coolant to determine its temperature distribution when drilling a rotating titanium workpiece. They also established a finite element model, and analyzed the data collected from the thermocouple using inverse heat transfer analysis, which verified the validity of the finite element model they proposed [37, 38].

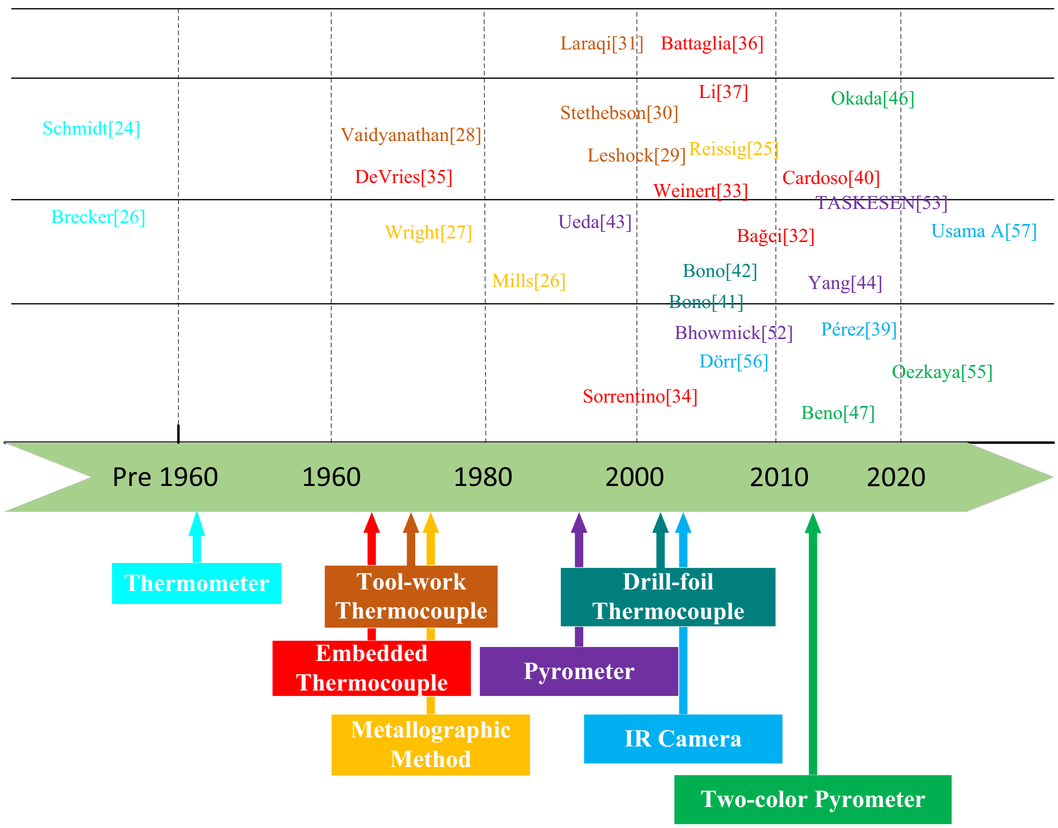

Figure 4 The development of different techniques for temperature measurement

Also, thermocouples can be embedded into a workpiece to study its temperature distribution. As the drill passed by each thermocouple, the friction between the drill and the workpiece raised the temperature of each thermocouple's immediate surroundings, creating electromotive force that were used to determined temperature distribution. In the research of Pérez et al., four thermocouples were embedded in the workpiece at different distances near the hole to measure the temperature to study the influence of process parameters and workpiece material properties on heat dissipation [39]. Cardoso et al. determined the heat flux and convection coefficient in drilling by using the inverse heat conduction method. What's more, three thermocouples were positioned at 3, 7 and 11 mm from the drill entrance to obtain the temperature gradient along the axis of the hole, as shown in Figure 7 [40].

3.1.3 Tool-Foil Thermocouple System

As shown in Figure 8, tool-foil thermocouple system proposed by Bono et al. can be regarded as a combination of a tool-work thermocouple system and an embedded thermocouple. During drilling process, the drill and foil can form a hot junction as the drill contacts the foil. When the drill and foil are connected to the cold reference junction, the thermoelectric circuit is closed to generate and collect a voltage proportional to the temperature [41]. Bono et al. later also used the tool-foil thermocouple system and combined a finite element model to study the temperature distribution on the cutting edge of the drill, research showed that the finite element simulation results were consistent with the experimental ones [42]. In Zhu's research, a tool-foil thermocouple system was also used to measure the temperature when drilling Al/Ti stacks. The research pointed out that the feed rate had a more obvious effect on the drilling temperature than the cutting speed, and the drilling temperature decreased from the center of the bit along the cutting edge [3].

3.2 Non-Contact Measurement Techniques

The above-mentioned method of using thermocouple measurement usually affects the heat flow and temperature gradient of the tool and the workpiece. On the contrary, the non-contact measurement obviously improves these shortcomings. For this reason, non-contact measurement methods are used because of the ability to

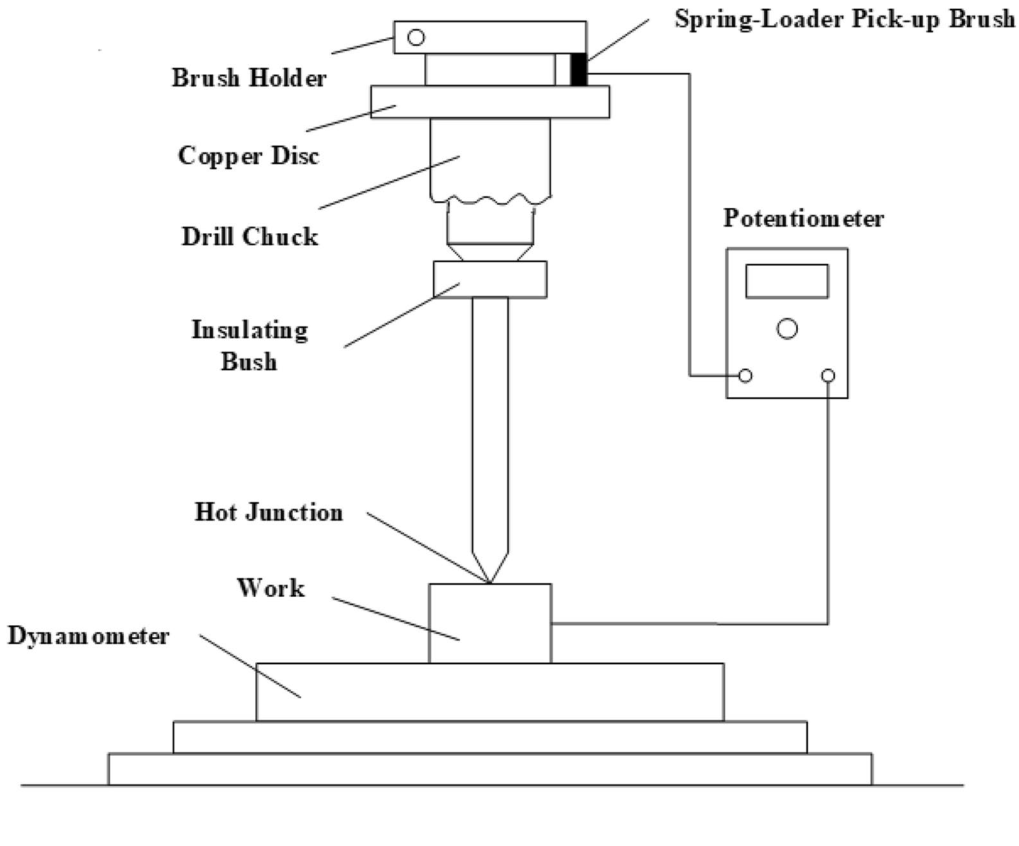

Figure 5 Tool-work Thermocouple [28]

obtain drilling temperature remotely. There are many non-contact measurement methods, but the methods used in drilling are completely limited to infrared radiation. Therefore, an optical pyrometer [43, 44], optical fiber two-color pyrometer [45–47] and infrared radiation camera [48–50] are generally used to measure drilling temperature.

According to Stefan-boltzmann's law, the temperature of the drill can be determined by measuring its thermal radiation, and the energy radiated by the object is proportional to the fourth power of the temperature. That is, $R=\varepsilon\sigma T^4$, where R is the energy radiated by the object, ε is the emissivity of the object, σ is the Stefan-boltzmann constant, and T is the kelvin temperature of the object [51].

3.2.1 Optical Pyrometer and Optical Fiber Two-Color Pyrometer

The optical pyrometer is the simplest radiation measurement device used in drilling research. It consists of a lens that focuses the infrared radiation on a single photosensitive cell. Then this cell generates a signal, which is amplified, processed, and then output to an LCD screen, computer or data logger. Bhowmick et al. used a pyrometer to measure the temperature when drilling magnesium alloy AM60. The research results showed that: compared with dry drilling, MQL drilling had a significantly lower maximum temperature on the workpiece, which can effectively improve the problem of material softening and reduce magnesium adhesion and built-up edge formation [52]. Taskesen et al. also used an optical pyrometer to measure the temperature of the drill. Due to the different distances from the measured object, the optical pyrometer has different spot diameters. Therefore, the optical pyrometer must be moved with the tool to keep the distance between the tool and the pyrometer and the diameter of the spot constant. For this purpose, as shown in Figure 9, one end of the fastening device was installed on the spindle of the machine tool, and the other end was fixed on the pyrometer [53]. When comparing the cooling effect of MQL and liquid carbon dioxide (LCO_2), Luka et al used a pyrometer to measure the temperature. The device is shown in Figure 10. The results showed that: LCO_2 proved more efficient at lower drilling

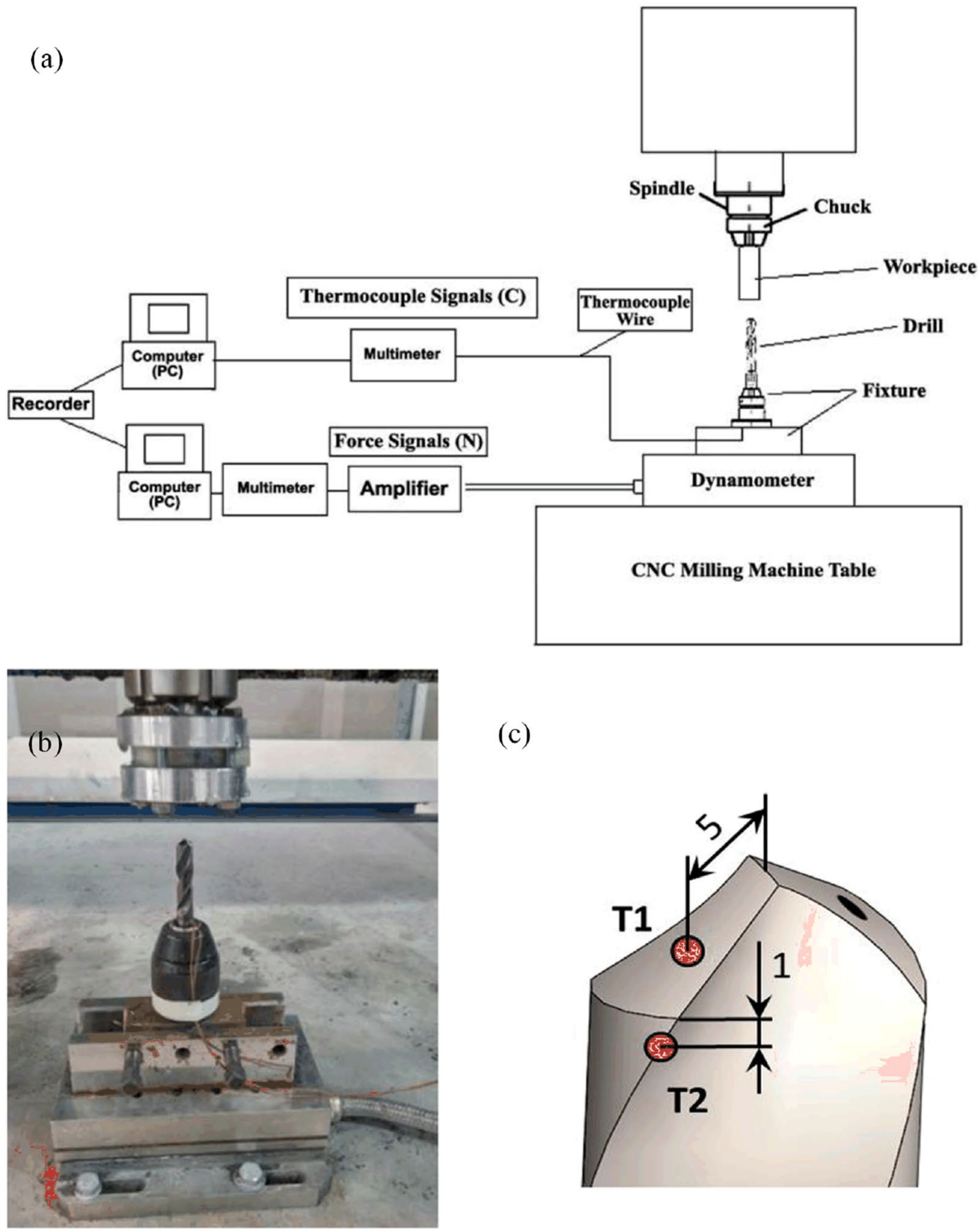

Figure 6 Thermocouple embedded in tool, **a** Schematic representation of experimental set-up, **b** The experimental set-up, **c** The thermocouple was inserted through the oil hole [32, 38]

temperatures and LCO_2+ MQL combination performed better in reducing temperature [54].

There are two photosensitive elements in the two-color pyrometer, and each element is sensitive to different wavelengths of infrared radiation. Consequently, the element only measures two specific wavelengths of infrared radiation, reducing errors in the measurement process. Oezkaya et al. measured the drilling temperature along the cutting edge by using a two-color fiber optic pyrometer (see Figure 11). The results showed that the increase in cutting speed and feed rate will significantly increase the temperature of the cutting edge corners while the temperature at the inner diameter of the tool remains almost unchanged [55].

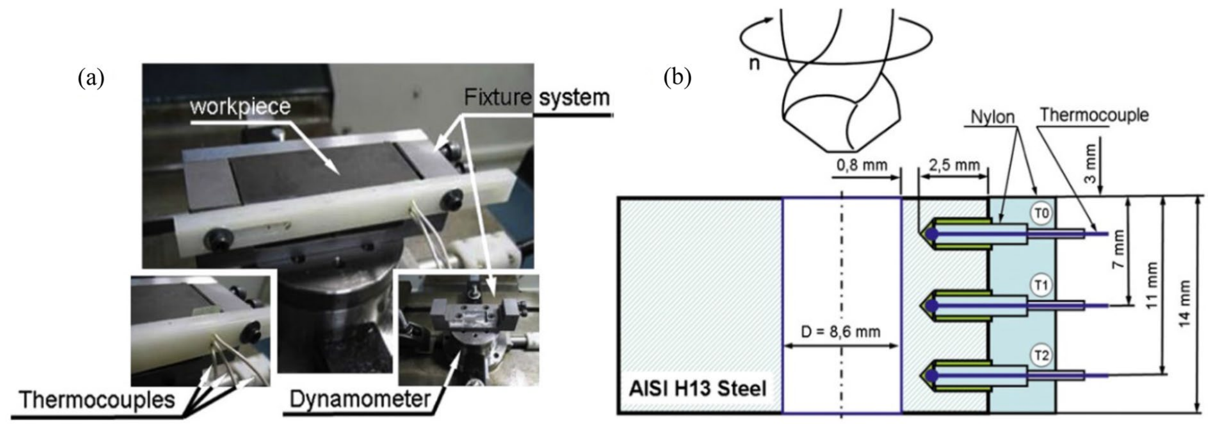

Figure 7 Thermocouple embedded into the workpiece **a** The experimental set-up, **b** Layout of the embedded thermocouples [40]

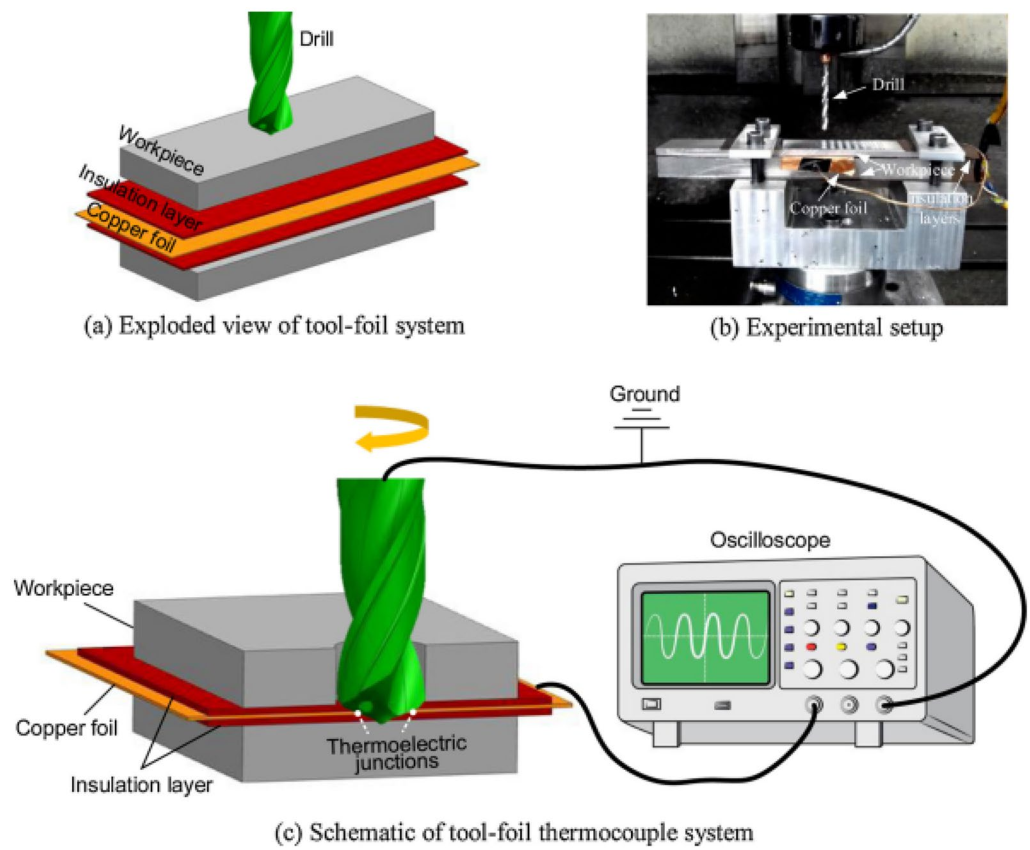

Figure 8 Schematic of tool-foil thermocouple system [3]

3.2.2 Infrared Camera

Infrared camera also plays an important role in non-contact measurement. By using special filters, lenses, microbolometer arrays or combinations thereof, infrared camera receive infrared radiation and measure its intensity. After processing the signal generated by the photosensitive cells, the camera generates thermal images of the target object, which are color-coded to represent different temperatures. Dörr et al. studied the performance of different drill coatings by using an infrared

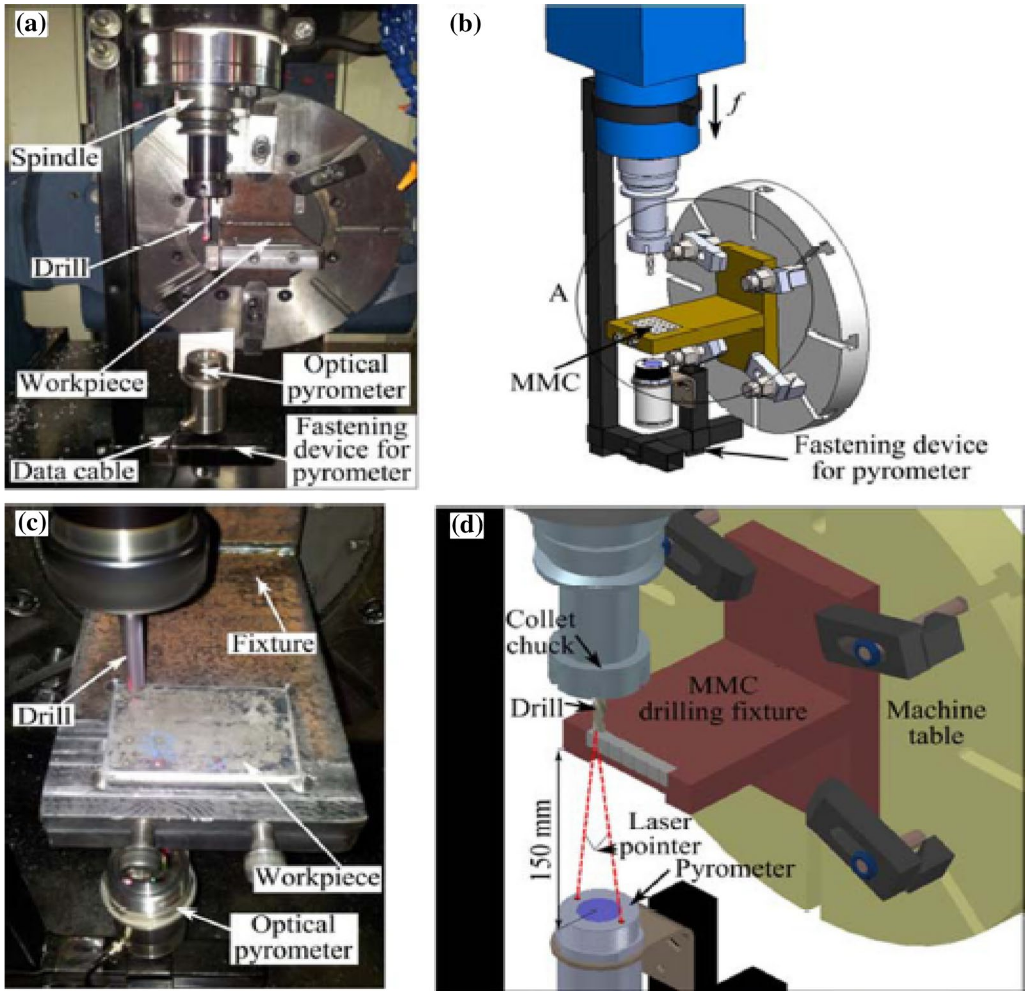

Figure 9 Test setup for temperature measurement: **a** Picture of test setup, **b** Solid model view of test setup, **c** Detail of A (Test setup), **d** Detail of A [53]

camera. In order to make sure optical access to the drilling site, a 45° deflection mirror was placed under the workpiece which can reflect the infrared radiation to the infrared camera from the drill's exit point, then the tool temperature was obtained. The result showed that it was possible to reduce the thermal stresses by using special coatings, thereby reducing tool wear and extending tool life [56]. However, when the drill is inside the workpiece, the infrared camera cannot detect the temperature of the drill. Therefore, the infrared camera usually needs to be used together with thermocouples in the drilling process. For example, Pérez et al. used thermocouples embedded in the workpiece and an infrared camera to study the effect of material properties and cutting speed on the heat dissipation of drilling CFRP [39]. Khashaba et al. used an infrared camera and two thermocouples installed in the internal coolant holes of the drill to study the heat affected zone (HAZ) and drill point temperature, as shown in Figure 12. The study pointed out that the thickness of the workpiece, the spindle speed and the feed rate all had a significant effect on the drilling temperature [57]. Bonnet et al. divided the drill into four parts, and calculated their heat flow according to the different cutting speeds and different working rake angles of the four parts during the drilling process, then measured the drilling temperature using an infrared camera, as shown in Figure 13 [17].

4 Effect of Process Parameters on Drilling Temperature

The process parameters, such as spindle speed and feed rate, directly participate in the entire machining process of the workpiece, which affect the temperature of the drilling process, and in turn affect the quality of

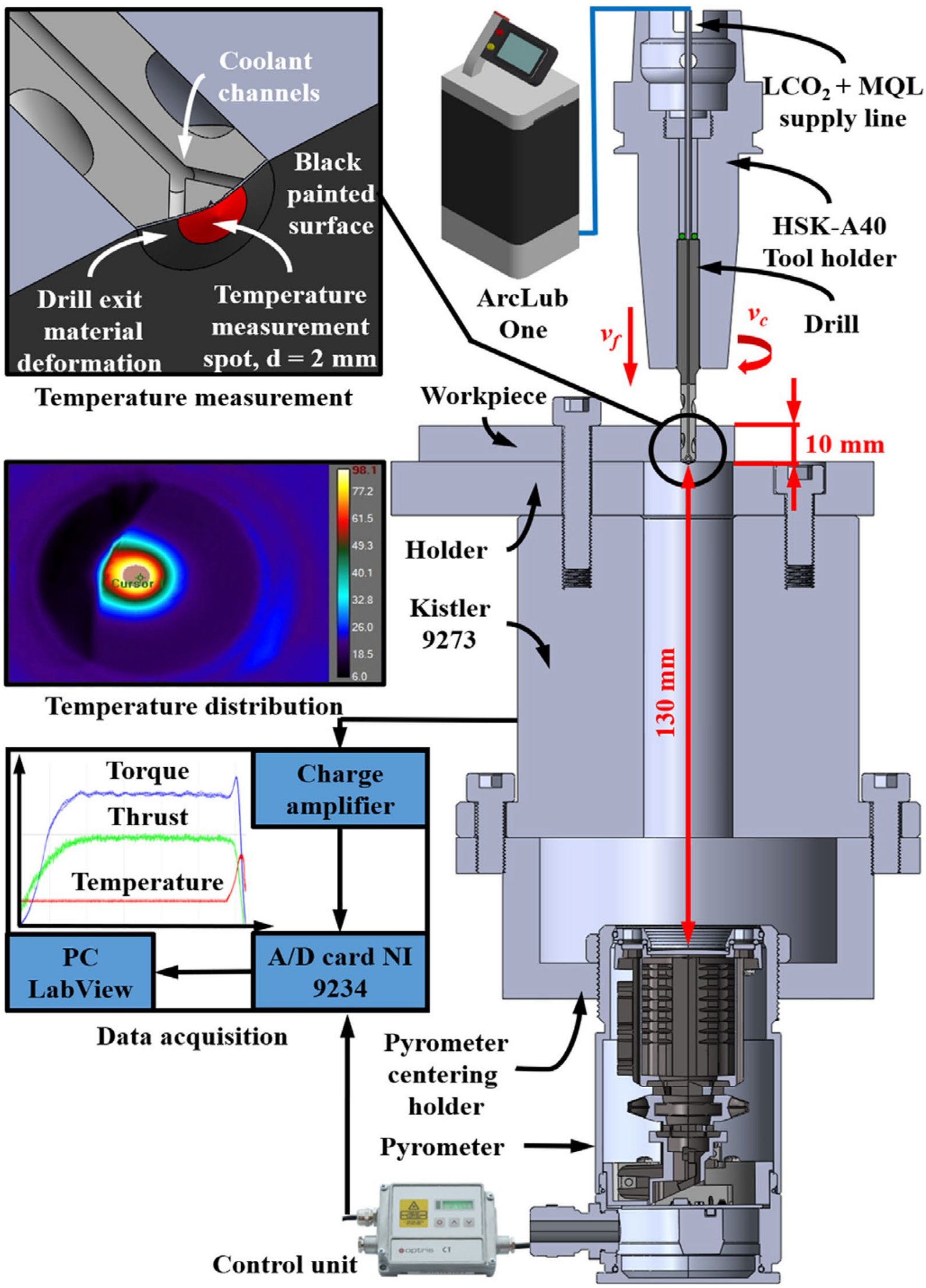

Figure 10 Illustration of the experimental setup [54]

the drilling [58–61]. And researchers have done a lot of research in this direction, which shows the importance of process parameters to control the drilling temperature.

4.1 Effect of Process Parameters During Drilling Metallic Materials

In Bağci's study of the temperature distribution of the tool, drilling temperature was measured by embedded

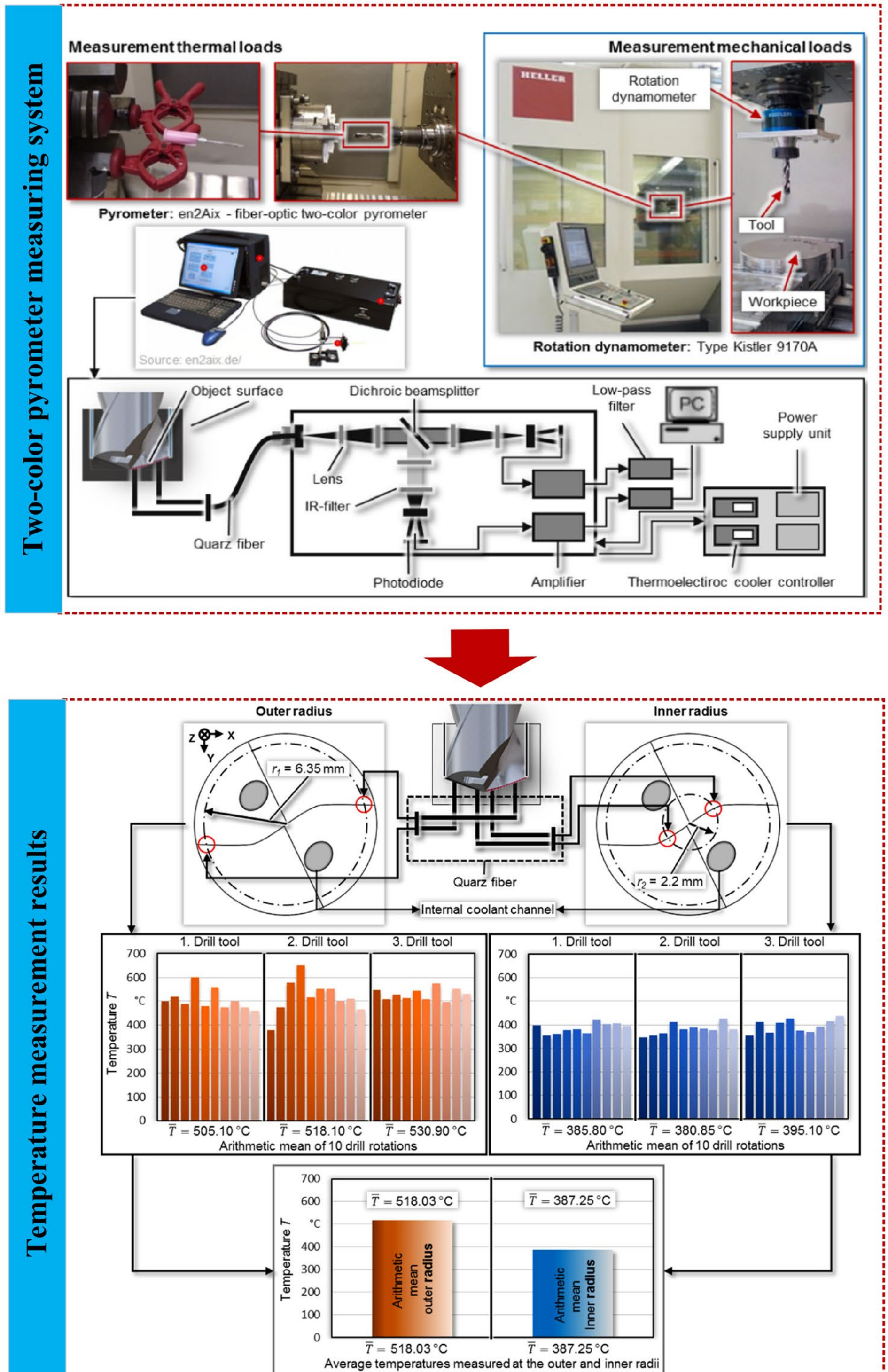

Figure 11 Two-color pyrometer temperature measuring system and temperature measurement result [55]

thermocouples through the oil hole of the drill. Experiments were conducted by using two different workpiece materials, Al 7075-T651 alloy and AISI 1040 steel. It was observed that the temperature decreased with the increase of the feed speed for the same drilling depth and spindle speed. Additionally, the temperature increased

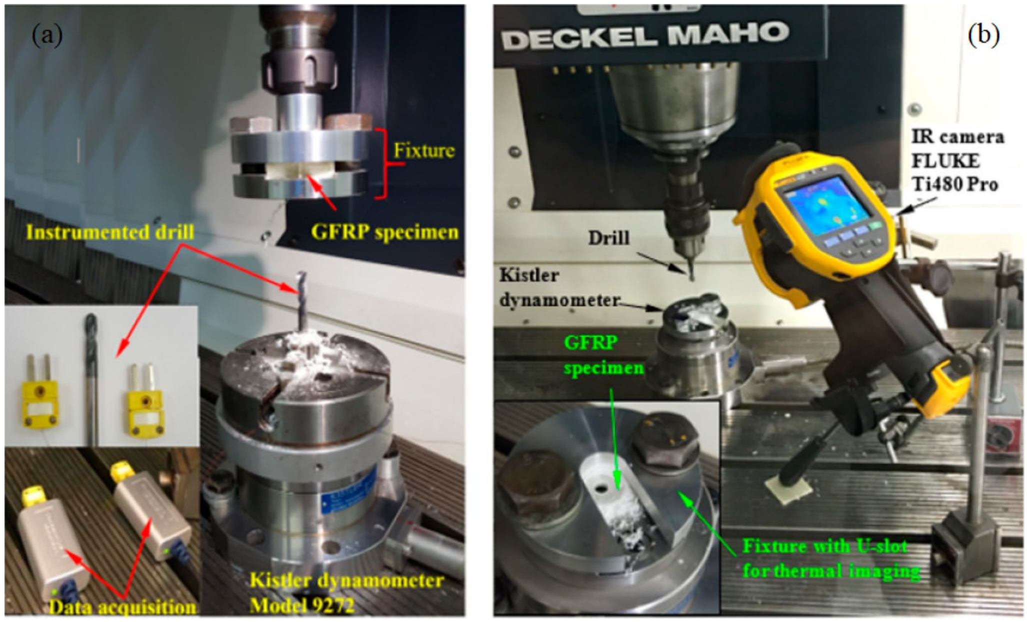

Figure 12 The temperature was measured by: **a** Instrumented drill with two thermocouples and **b** IR camera [57]

on the drill with the increase of the spindle speed for the same feed rate during drilling AISI 1040 steel, while the temperature decreased with the increase of the spindle speed for Al 7075-T651 materials [62]. In the study of drilling AISI 1045, the conclusion presented that as the spindle speed and feed rate increased, the drilling temperature also increased [63, 64]. Parida et al. observed that torque and thrust increased with the increase of the cutting speed, which in turn increased the drilling temperature when drilling Ti-6Al-4V at a low cutting speed; However, the opposite results were observed at a high cutting speed because the increase of cutting speed reduced the hardness of workpiece due to thermal softening, as a result, reducing the drilling temperature [65, 66]. Although the experimental conditions may be different, the trend of the influence on drilling temperature was similar, that is, as the feed speed and cutting speed increased, the drilling temperature increased when drilling aluminum alloys and magnesium alloys [3, 67, 68]. Figure 14 shows the effect of process parameters on drilling temperature when drilling different metal materials.

4.2 Effect of Process Parameters During Drilling GFRP and CFRP

Ünal and Xu have studied the drilling temperature characteristics of glass-fiber reinforced plastic (GFRP) and CFRP respectively. From their experimental results, no matter which materials they drilled, the drilling temperature increased with the increase of the cutting speed and feed rate. The reason was that as the feed rate increased, the contact time between the tool and the workpiece will be shortened, which led to a reduction in the heat generated by friction and thus lowered the drilling temperature. What's more, as the cutting speed increased, the cutting area per unit time will be longer, so that the drilling temperature will be higher [69, 70]. In the research on drilling CFRP, Chen et al. pointed out that low spindle speed and high feed rate can effectively reduce the generation of cutting heat when the spindle speed was in the range of 1500–4500 r/min and the feed rate increased from 0.02 to 0.06 mm/rev. However, low spindle speed and high feed rate will increase the cutting force, which may increase the possibility of delamination defects in CFRP drilling. Therefore, while paying attention to how to suppress the cutting heat, the dialectical relationship between the feed rate and cutting speed, cutting force and cutting heat should be considered, and the processing parameters should be selected reasonably [71]. Figures 15 and 16 show the effect of process parameters on drilling temperature when drilling CFRP and GFRP. Zitoune's research showed that the drilling temperature increased with the increase of the feed rate, while the cutting speed had a relatively small effect on the drilling temperature when drilling CFRP [72].

4.3 Effect of Process Parameters During Drilling Laminated Materials

An et al. pointed out that the drilling temperature will increase with the increase of feed rate and cutting speed, and the cutting speed had a more significant influence

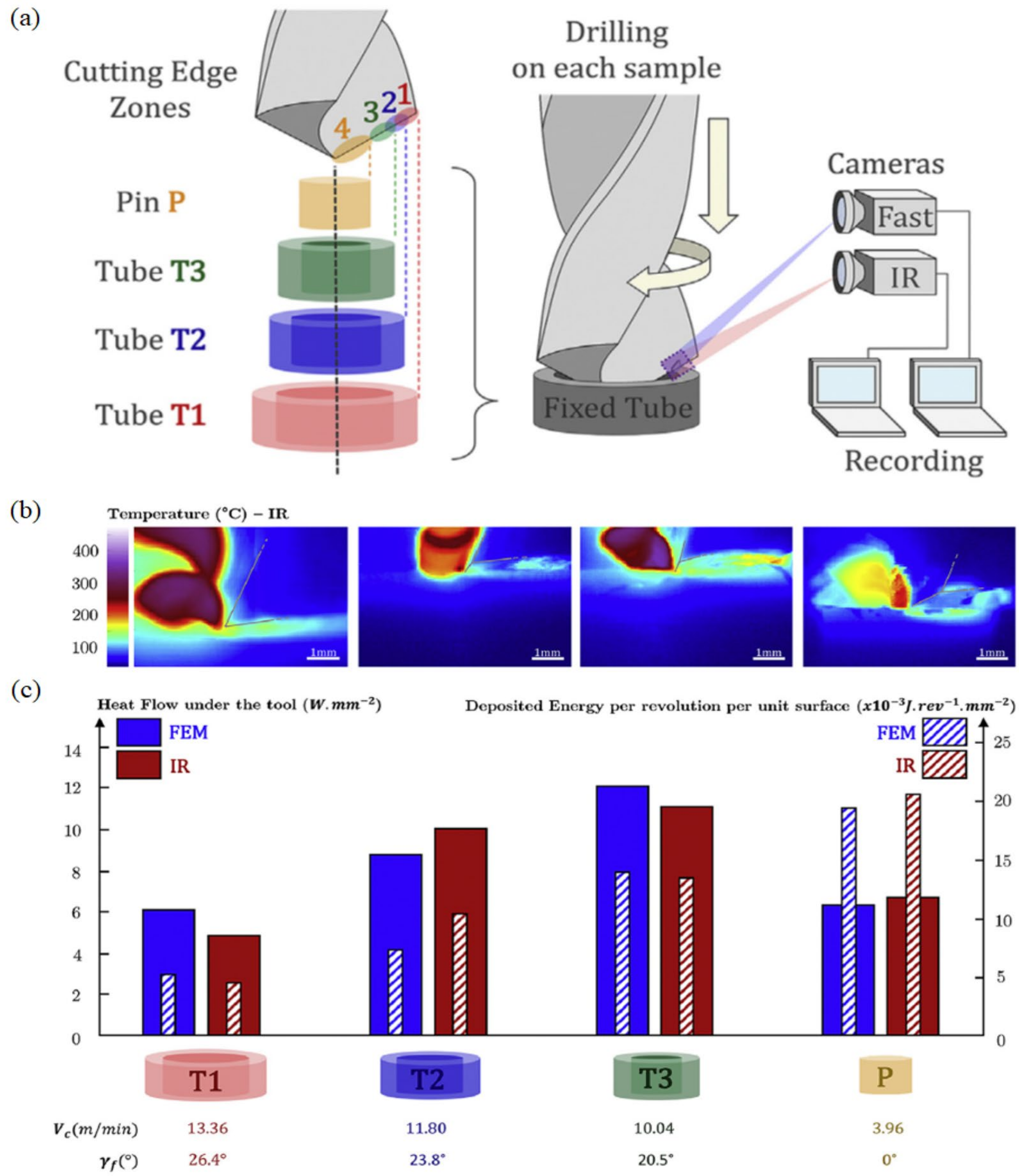

Figure 13 Measuring cutting heat by using IR camera: **a** Experimental set-up, **b** IR Temperature, **c** Heat Flow under the tool and deposited energy per rev per unit of the workpiece surface [17]

on the drilling temperature than the feed speed whether drilling the stacks from the CFRP layer or Ti-6Al-4V layer when drilling CFRP/Ti stacks. Furthermore, the maximum temperature when drilling the stacks from the CFRP layer was also 2%–14% higher than the maximum temperature when drilling the stacks from the Ti-6Al-4V layer [73]. Figure 17 shows the effect of process parameters on drilling temperature when drilling CFRP/Ti stacks.

Weinert et al. found that the cutting speed was positively correlated with the flank surface temperature of the tool when the cutting speed was in the range of 35–200 m/min and Chen also obtained the same conclusion in his research [33, 74]. In contrast, Rawat et al. pointed out that as the feed rate increased, the flank surface of the tool showed a decrease in temperature [75]. Sorrentino et al. combined numerical analysis and experiment to predict the trend of temperature with spindle speed and feed rate during the drilling process. The results showed that the maximum temperature of the tool was positively correlated with the spindle speed and negatively correlated with the feed rate. For the

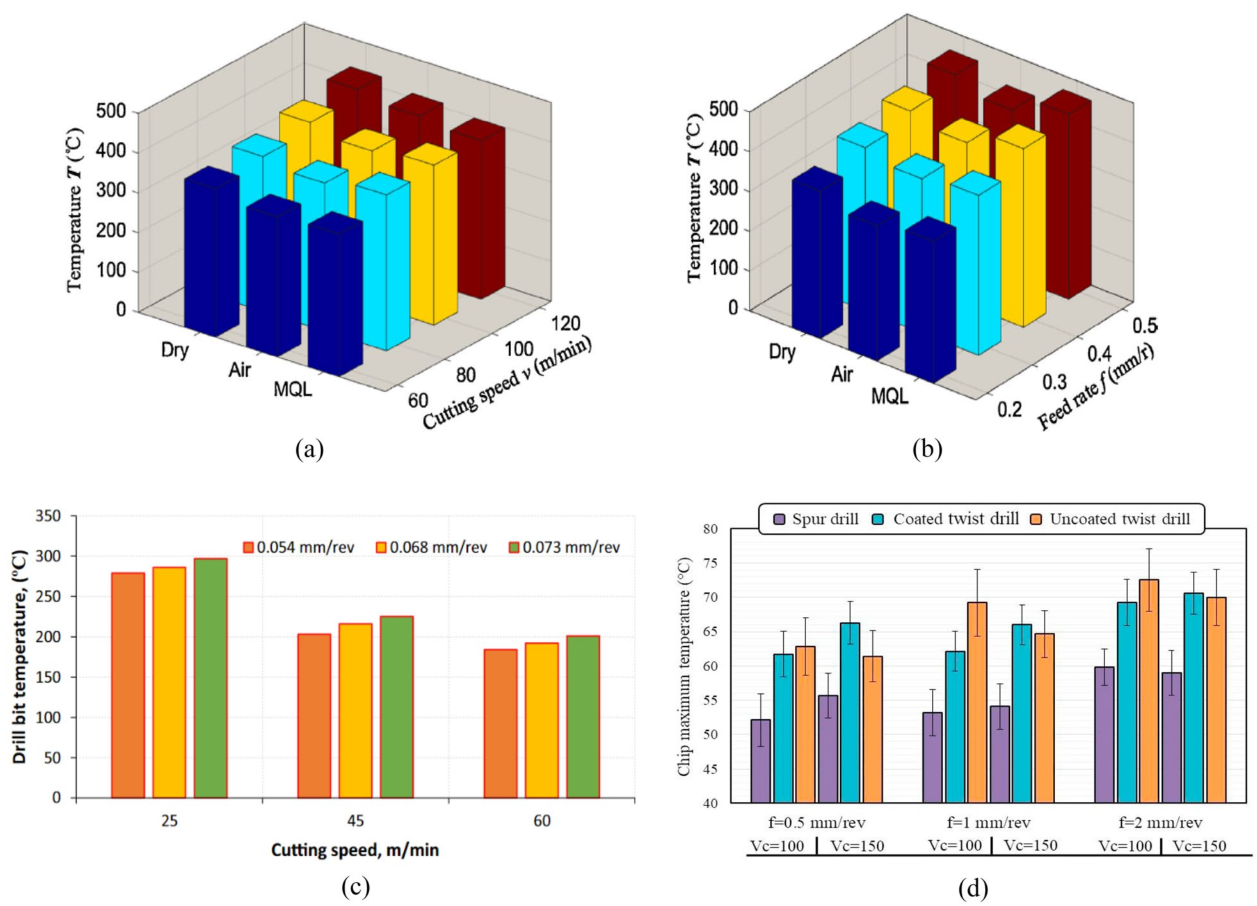

Figure 14 Temperature for different drilling conditions: **a**, **b** When drilling Aluminum alloy, **c** When drilling Ti-6Al-4V, **d** When drilling Magnesium alloy [3, 66, 67]

corresponding workpiece, when drilling at the low-speed, the temperature decreased with the increase of the feed rate, while at the high-speed, the temperature of the workpiece was almost constant [76].

It can be seen from the above research that, in the drilling process, the process parameters and the drilling temperature are not simply linear, and their impact on the hole quality is not simply a linear superposition. It should be noted that the selected tool material, workpiece material, cooling process, etc. are all important factors that affect the correlation mechanism between process parameters and drilling temperature. Therefore, it needs more in-depth and systematic exploration to accurately grasp the correlation mechanism between process parameters and drilling temperature.

5 Effect of Tool Geometries on Drilling Temperature

Scholars have done a lot of research on the improvement of the tool geometries [77–81], but there are relatively few studies on the influence of the tool geometries on the drilling temperature. For drilling processing, the optimization and improvement of the tool geometries are conducive to improving the drilling temperature, realizing high-efficiency and high-quality processing, increasing tool life and reducing processing costs. Therefore, the reasonable design of the tool geometries is also very important to reduce the cutting heat.

5.1 Effect of Point Angle and Helical Angle on Drilling Temperature

Liang et al. conducted simulation analysis and experiments on the cutting heat of conventional drilling and ultrasonic vibration-assisted drilling under different tool point angles. The results showed that compared with conventional drilling(CD), cutting heat can be

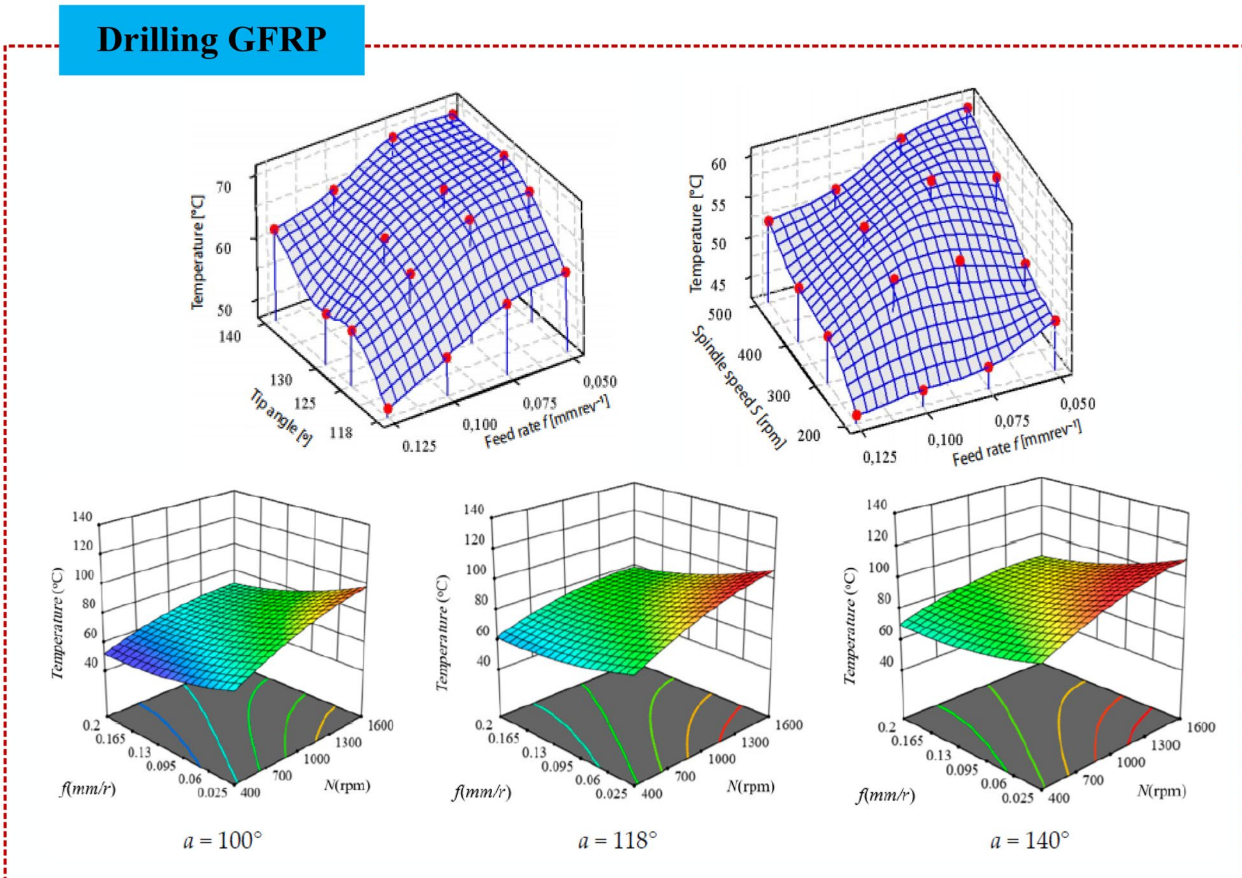

Figure 15 Drilling temperature when drilling GFRP [57, 69]

reduced significantly in ultrasonic vibration-assisted drilling(UAD). Additionally, as the tool point angle increased, the drilling temperature will also increase, and a proper point angle had a significant effect on reducing burr height and surface roughness, as shown in Figure 18 [82]. Kumar et al. explored the impact of tool geometries on the chip removal ability and tool wear. It was found that the drill with 130° point angle, 30° helix angle and smaller chisel edge thickness had less wear on the flank face and chisel edge, and the chips were easier to discharge. On the contrary, for the drill with 118° point angle, 20° helix angle and a larger chisel edge thickness, the local plastic deformation of the workpiece and the tool wear were more serious. In addition, this drill increased the contact area between the tool and the workpiece, which increased the friction and then the drilling temperature also rose [83]. Yao et al. analyzed the drilling temperature using low-frequency vibration drilling. The experimental results showed that the point angle, helix angle of the drill had little effect on the temperature of low-frequency vibration drilling. Because the vibration can make the tool periodically leave the machining surface of the workpiece, and then the tool was cooled after being in contact with air. Additionally, titanium alloy chips have changed from band-shaped chips in traditional drilling to chip-shaped chips, which can be discharged from the spiral groove with the rotation of the tool during the drilling process and take away a large amount of cutting heat. Therefore, low-frequency vibration drilling can control the temperature at a lower level, and the influence of the geometric parameters of the tool on the drilling temperature can be ignored [84].

Fuh et al. revealed some important thermal phenomena related to the tool geometries, for example, the helix angle was positively related to the drilling temperature and as the web thickness became thicker, the drilling temperature decreased [13]. Chen and Wang et al. pointed out that the increase in the helix angle caused the increase of the rake angle, which led to the reduction of the friction between the chip and the rake surface, and the drilling temperature decreased accordingly [74, 85]. It can be seen that they have obtained different results on

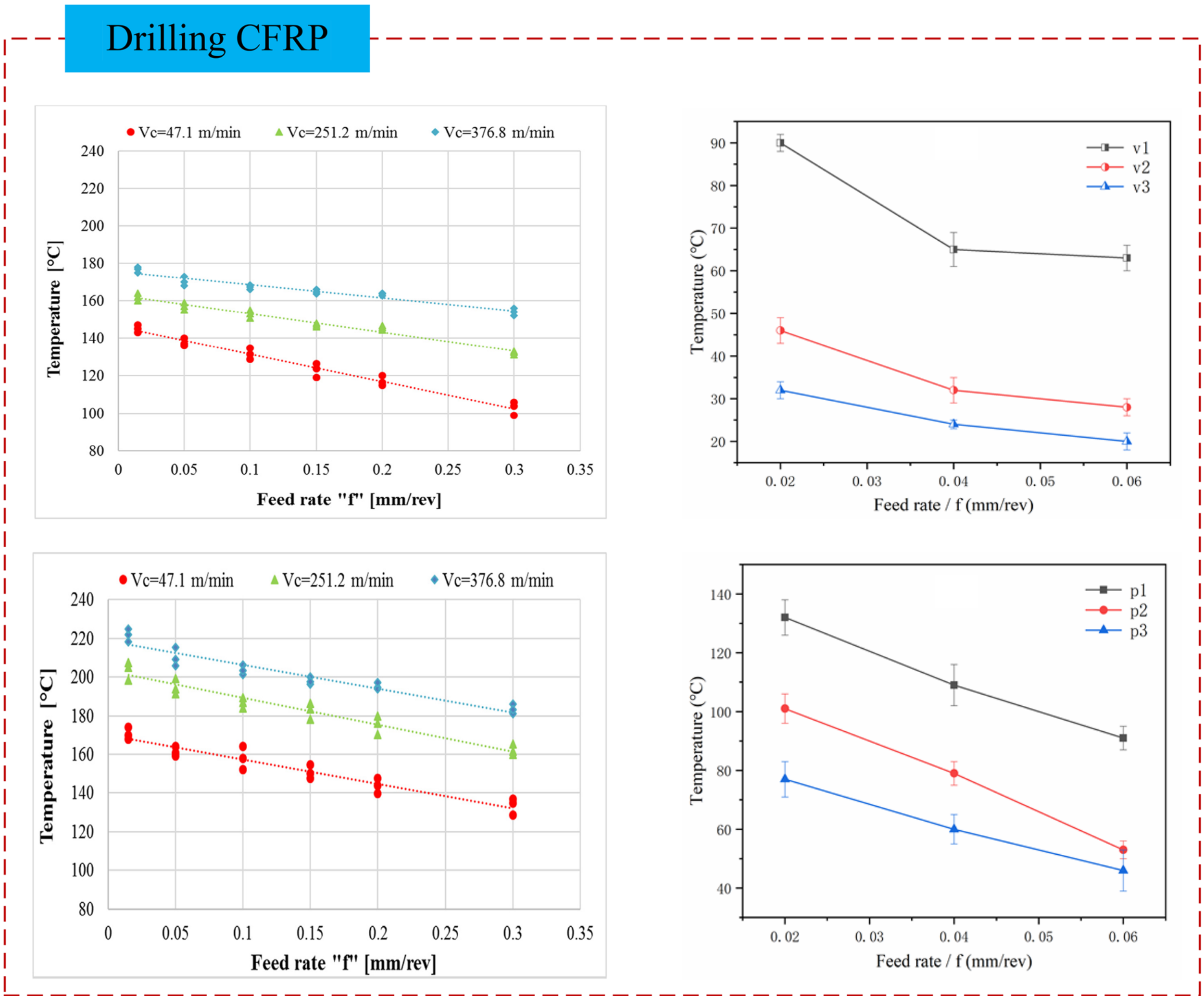

Figure 16 Drilling temperature when drilling CFRP [34, 71]

the effect of the helix angle on the drilling temperature. The reason for this phenomenon may be due to different workpiece materials and different cutting parameters. In addition, as the helix angle changed, the shape of the chips also changed, which affected chip discharge and thus affected the drilling temperature [86, 87]. Therefore, in my opinion, the mechanism of the influence of the helix angle on the drilling temperature needs more in-depth research.

5.2 Effect of Macro/Micro Tool Geometries on Drilling Temperature

Sugita et al. proposed a novel drill design with a thinner cutting edge and chisel edge which will shape the tool compared with a twist drill. Therefore, during the drilling process, the cutting force was lower than that of twist drill, which led to a reduction in cutting heat. Furthermore, due to its special structure, the drill had a stronger chip removal performance, which helped to dissipate heat [88]. Shu et al. designed a novel drill for drilling CFRP. As shown in Figure 19, the web and lip thinning design will efficiently increase the rake angle and change the material removal mechanism of CFRP from compression and tensile fracture to shearing cutting and compression shear, which had a significant reduction on the drilling temperature and cutting force. In addition, as we know, the elevation in cutting force and temperature have an impact on the exit delamination and micro-damage of the hole wall. Therefore, the novel drill with superior thermo-mechanical properties can effectively achieve CFRP damage-free drilling of CFPR [89–92].

Chen et al. applied the 3D finite element method to analyze two drill bits with different cross-sectional shapes, and obtained the temperature distribution. The

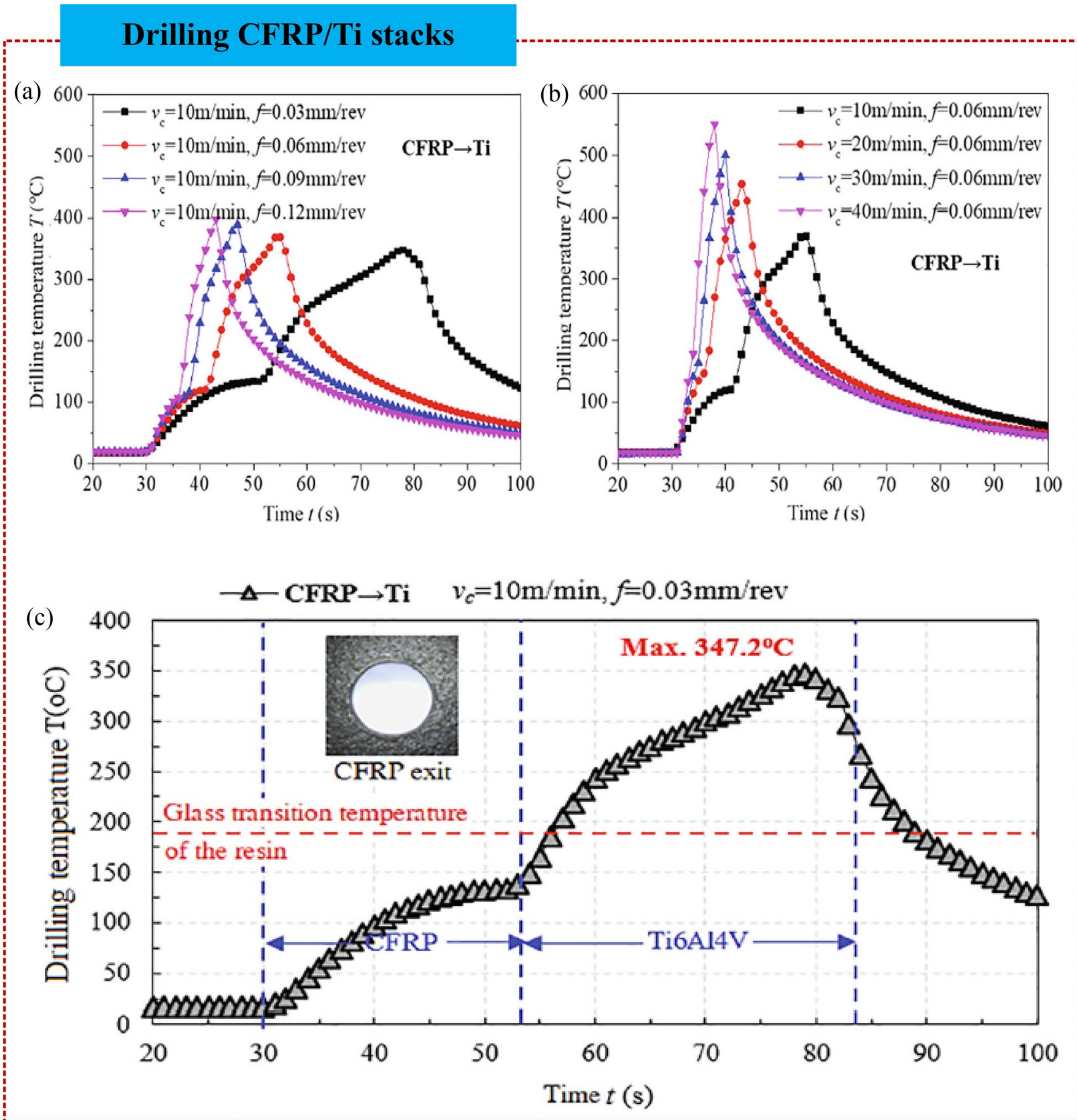

Figure 17 Drilling temperature when drilling CFRP/Ti stacks [73]

results showed that the thick web drill with a curved cutting edge had a more uniform and lower temperature distribution along the edge and flank surface than the thick web drill with a straight cutting edge [93]. Müller et al. designed different groove-shape structures on the first rake face of the drill to improve the cooling efficiency. The results showed that different groove structures can change the heat flow rate to achieve faster heat dissipation, and the cooling efficiency of different groove shapes was also different [94]. Pang et al. used the finite element method to analyze the performance of three different micro-textured drills, namely pit micro-textured, convex micro-textured and grooved micro-textured drill in reducing the drilling temperature. The results showed that the drilling temperature of the micro-textured drill was lower than that of the conventional drill. This was

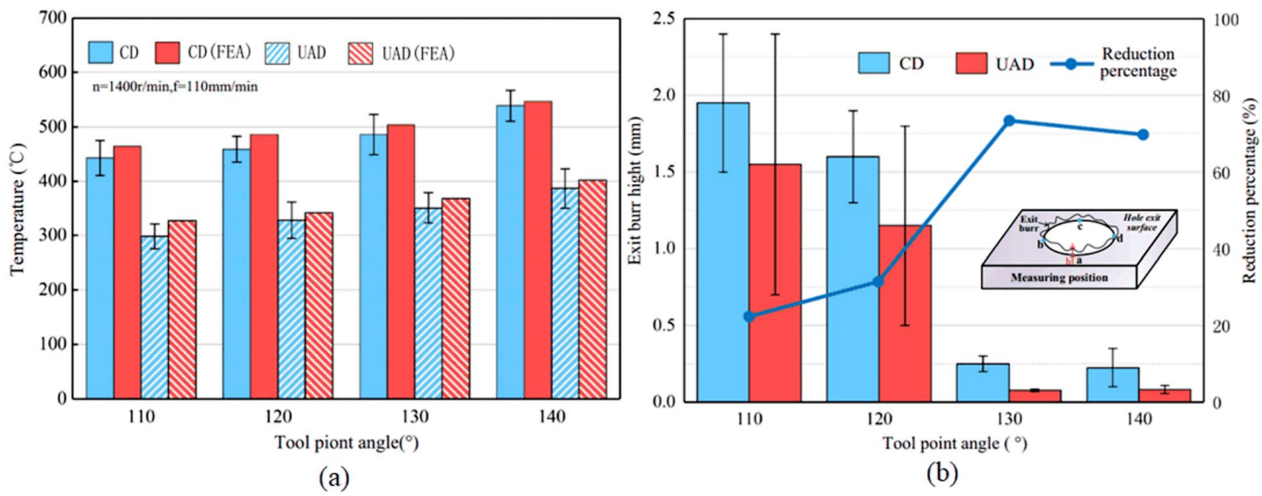

Figure 18 Influence of point Angle on drilling temperature and burr height: **a** comparison of cutting heat between CD and UAD, **b** comparison of exit burr height and reduction percentage between CD and UAD [82]

because the micro-textured drill reduced the actual contact area between the tool and the chip which will reduce the cutting heat generated by the friction, and the cooling effect of the groove micro-textured tool was stronger than that of the convex micro-textured tool, as shown in Figure 20 [95]. Wika et al. studied the impact of drills with different helix angles and different numbers of flutes on the temperature when drilling CFRP/Ti stacks. The research showed that the drilling temperature of the double-flute drill with large helix angle was lower than that of the three-flute drill with small helix angle. This was due to the double-flute drill with large helix angle had a strong chip removal ability and a sharper cutting edge, which was conducive to heat dissipation compared with the three-flute drill with small helix angle [96].

6 Effect of Different Hole-Making Methods on Drilling Temperature

In addition to traditional drilling methods, hole making methods also include low-frequency vibration-assisted drilling (LF-VAD) [97–99], ultrasonic vibration-assisted drilling (UAD) [100–102], orbital drilling [103–105] and laser drilling [106–108] etc. Due to the different methods of making holes, the mechanism of the influence on drilling temperature also needs to be analyzed separately. Although the existing literatures have conducted a lot of research on different hole making methods, they rarely give a systematic explanation of the effect of hole making methods on drilling temperature. Therefore, the work of this chapter is to link the work of different researchers and conduct a scientific and systematic analysis.

6.1 Effect of Low Frequency Vibration-Assisted on Drilling Temperature

LF-VAD can be regarded as superimposing an axial harmonic motion at the vibration frequency below 200 Hz on the basis of conventional drilling, which can effectively reduce the drilling temperature, improve surface integrity and facilitate chip breaking and chip removal (see Figure 21) [109–111], while conventional drilling showed a higher chip-rake face friction, higher drilling temperature, and poor chip removal mechanism.

Research by Okamura et al. found that LF-VAD with an amplitude of 0.4 mm and a frequency of 30 Hz can effectively control chip formation, greatly reducing the drilling temperature, tool wear and burr height at the hole exit [112]. Okamura et al. established an LF-VAD temperature model to determine the drilling temperature during the drilling and non-drilling periods. Due to the influence of the low-frequency vibration, the drilling tool periodically separated from the workpiece, resulting in the repeated rise and fall of the drilling temperature. The study showed that the simulated drilling temperature was in good agreement with the experimental results at the rising stage. However, in the dropping stage, because the friction heat, that is between the drill side and the inner surface of the hole, and the high-temperature chips accumulated in the drill flute were not considered, the simulated drilling temperature during the non-drilling period was significantly different from the experimental results [113]. When drilling CFRP/Ti stacks, Pecat et al. found that LFVAD can significantly improve borehole quality compared with conventional drilling. Additionally, it was observed that LF-VAD can achieve a sufficient chip extraction which can effectively prevent

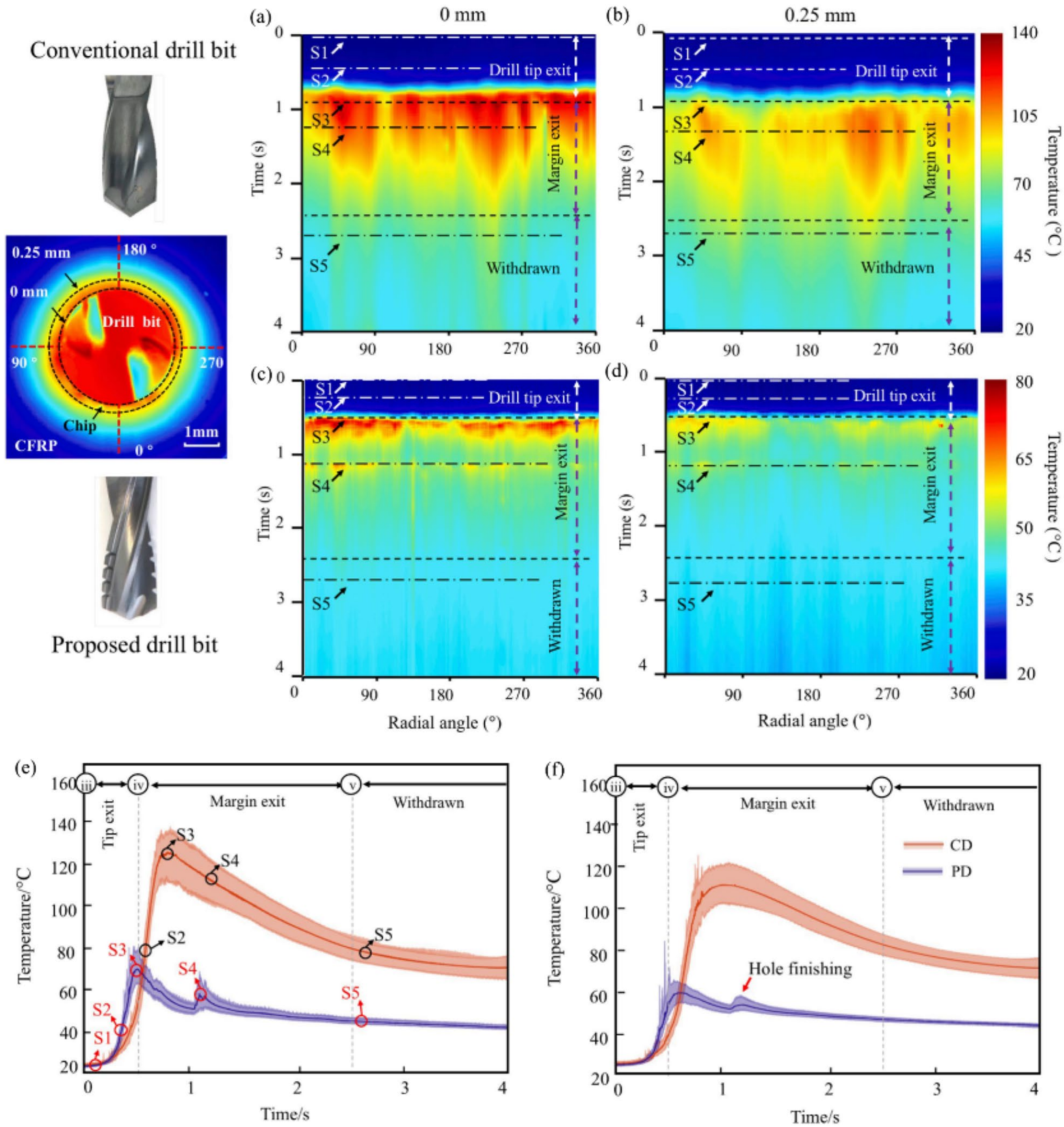

Figure 19 The temperature variations using the CD and PD bits at 0 mm and 0.25 mm from the hole wall: **a**, **b** Two-dimensional temperature at 0 mm and 0.25 mm using CD bits, **c**, **d** Two-dimensional temperature at 0 mm and 0.25 mm using PD bits, **e**, **f** Comparison of temperature variations between CD and PD at 0 mm and 0.25 mm [91]

the thermo-mechanical damages at the borehole surface [114, 115]. Hussein et al. studied the influence of different machining parameters, such as feed rate, cutting speed modulation frequency and modulation amplitude, on the drilling temperature by using LF-VAD. The experimental results showed that a lower feed rate of 0.025 mm/rev and amplitude in the range of 0.1–0.24 mm can greatly reduce the drilling temperature, and the amplitude had the most significant effect on the drilling temperature. In addition, due to the reduction of drilling temperature and the enhancement of chip removal ability, LF-VAD largely eliminated the delamination defect of the entry and the

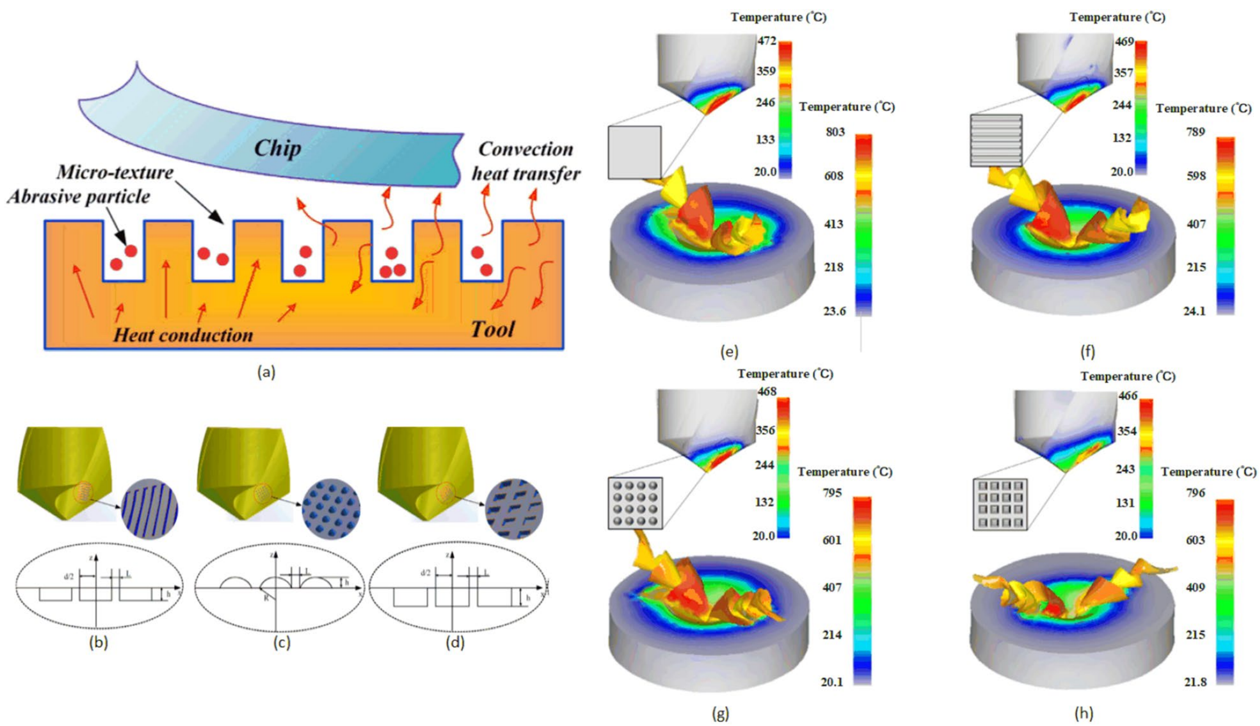

Figure 20 The research on drilling temperature with differently micro-textured drilling tools: **a** Schematic diagram of micro-texture anti-friction and heat conduction mechanism, **b**–**d** Micro-texture section shape of drilling tools of grooved micro- texture, convex micro-texture and pit micro-texture, **e**–**h** Temperature distribution of drilling process with non-micro-textured drilling tool and different micro-textured drilling tool [95]

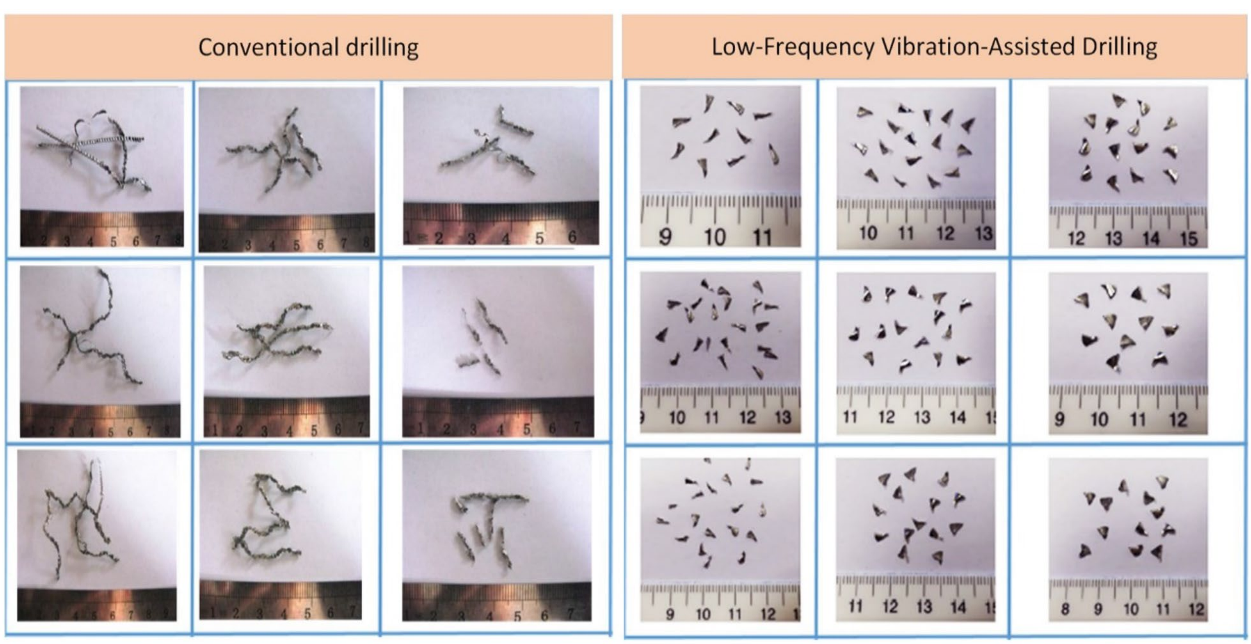

Figure 21 Chip morphology in conventional drilling and LFVAD [110, 111]

exit [116]. In the experiment comparing conventional drilling and LF-VAD, Yao et al. found that a larger amplitude can lower the drilling temperature, and improve the hole quality and chip removal performance. However, as the amplitude increased, the axial force also increased, which was likely to cause delamination defects. Therefore, various factors should be considered comprehensively to obtain better hole-making quality [117]. Sadek et al. found that LF-VAD can reduce the thermal and mechanical defects associated with CFRP compared with conventional drilling (Figure 22). In this study, the optimized low-frequency vibration conditions can reduce the axial force by 40% and the drilling temperature by 50% without causing delamination defects [118].

6.2 Effect of Ultrasonic Vibration-Assisted on Drilling Temperature

The UAD trajectory is composed of the high-speed rotation t, the feed motion and the ultrasonic vibration of the tool at a vibration frequency above 16 kHz, and its trajectory is shown in Figure 23. A large number of studies have proved that UAD can help solve the problem of drilling difficult-to-machine materials, so the technology has been widely used in the field of drilling.

Li and Liao et al. found that in UAD, the high amplitude was beneficial to enhance chip removal efficiency, and can effectively reduce the friction of the tool-workpiece interface, thereby reducing thrust and drilling temperature [119, 120]. In order to explore the effect of UAD on the temperature of the CFRP-Ti stacks interface, a thermocouple was placed near the stacks interface to measure the temperature, as shown in Figure 24. The experimental results showed that, in Ti6Al4V drilling stage, the drilling temperature of both conventional drilling and UAD rose rapidly and far exceeded the matrix glass transition temperature, which explained that drilling of the Ti6Al4V was the main reason for the thermal damage of CFRP [121, 122], and Sanda et al. came to the same conclusion [123]. This was due to the periodic contact and separation between the tool and the workpiece during the drilling process, which can effectively reduce the friction of the tool-workpiece interface, increase the cooling time of the drill, and effectively avoid the accumulation of cutting heat [124]. Li et al. came up with the following conclusions: most of the titanium alloy chips produced by conventional drilling and UAD were continuous banded chips, while the chips of LF-VAD and ultrasonic and low frequency compound vibration drilling were discontinuous sector-shaped chips. However, the chip size of ultrasonic and low frequency compound vibration drilling was smaller compared with LF-VAD which led to better heat dissipation performance [125].

Cong et al. explored the effects of ultrasonic power, cutting speed and feed rate on drilling temperature when ultrasonic vibration-assisted drilling of CFRP. The experimental results were shown in Figure 25, and it could be found that the maximum drilling temperature decreased with the ultrasonic power and feed rate. However, as the cutting speed increased, the maximum drilling temperature first climbed up and then declined [126]. Makhdum et al. conducted a comparative experiment between UAD and conventional drilling on CFRP, and found that the temperature of UAD was much higher than that of conventional drilling. This was mainly due to the repeated impact of UAD which inevitably led to temperature rise in the tool-workpiece interface. In other words, as long as the tool and workpiece separation occurred in each vibratory cycle, the local temperature will be affected by the imposed vibrations [127]. In Pujana's research, it pointed out that although the use of ultrasonic vibration to drill Ti6Al4V can reduce the feed force while the drilling temperature was higher than that of conventional drilling, and Yan also verified this conclusion through the finite element method [128, 129]. Moghaddas et al. explored the influence of ultrasonic vibrations on the drilling temperature in the UAD of stainless steel 316, alloy steel 4340 and aluminum 6061. The results illustrated that the increase in vibration amplitude resulted in a significant reduction in force and a higher drilling temperature [130].

6.3 Effect of Orbital Drilling on Drilling Temperature

Orbital drilling is also called helical milling. Its tool path is composed of three independent motions, which are the rotary motion of the tool itself, the orbital motion around the axis of hole and the feed motion. The trajectory of the tool is spiral, as shown in Figure 26 [131, 132]. Due to the special processing form of orbital drilling, it will not produce continuous chips like conventional drilling. Furthermore, the diameter of the tool is smaller than the hole diameter, so the chip removal ability performs better which leads to better heat dissipation compared with conventional drilling [133].

Comparing orbital drilling with conventional drilling, it is found that orbital drilling can effectively reduce the cutting temperature and axial force, and improve the surface quality. In the conventional drilling process, there are 2-4 cutting edges cutting at the same time while the orbital drilling has only one cutting edge in instantaneous contact with the tool-work interface which can obviously lower the axial force. What's more, the cooling effect of the rotating airflow between the tool and the workpiece and the excellent chip removal ability of the helical milling can effectively control the drilling temperature. Additionally, the reduction in drilling temperature and cutting

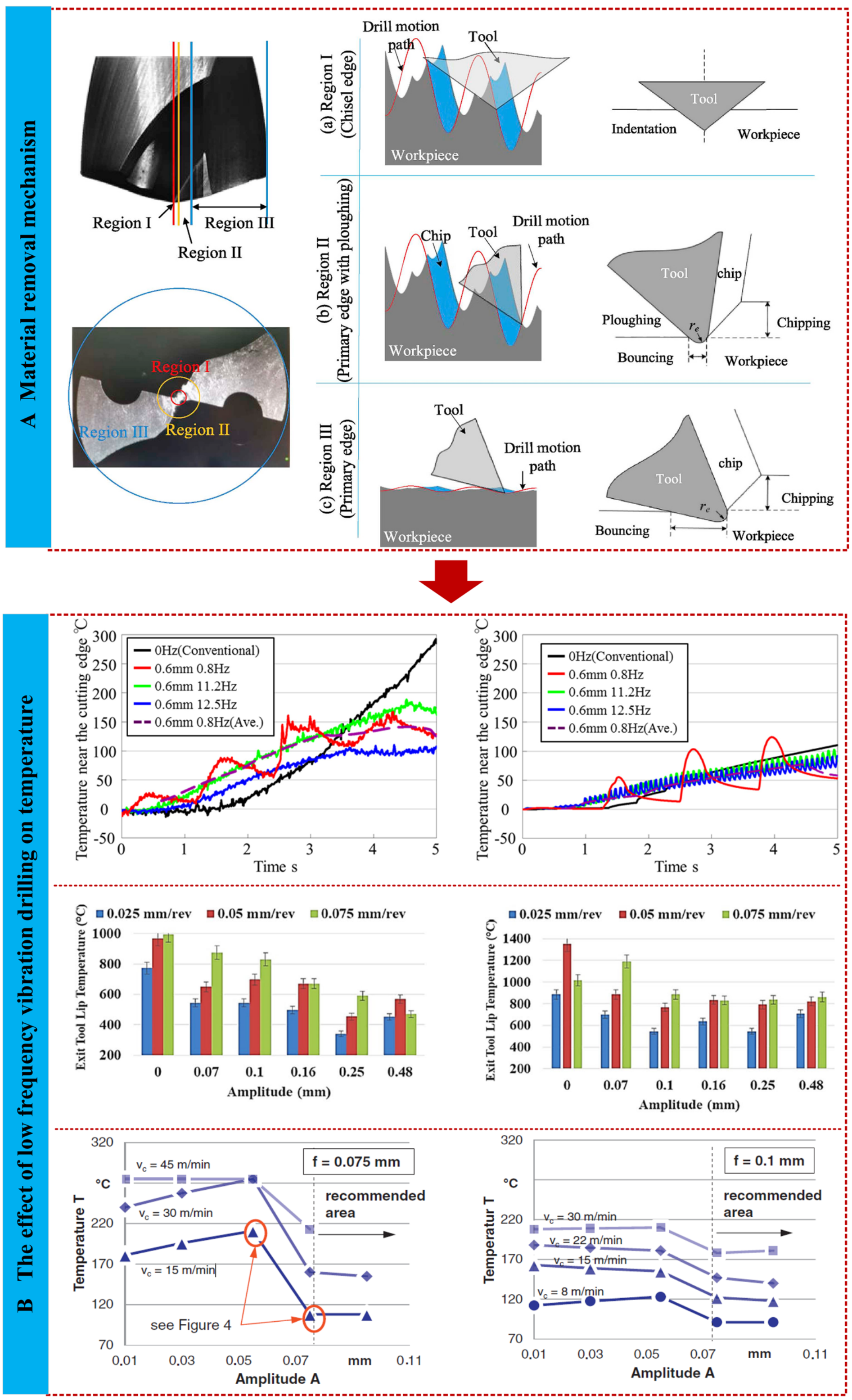

Figure 22 **A** is material removal behaviors within different regions, **B** is the effect of low frequency vibration drilling on temperature [109, 113, 115, 116]

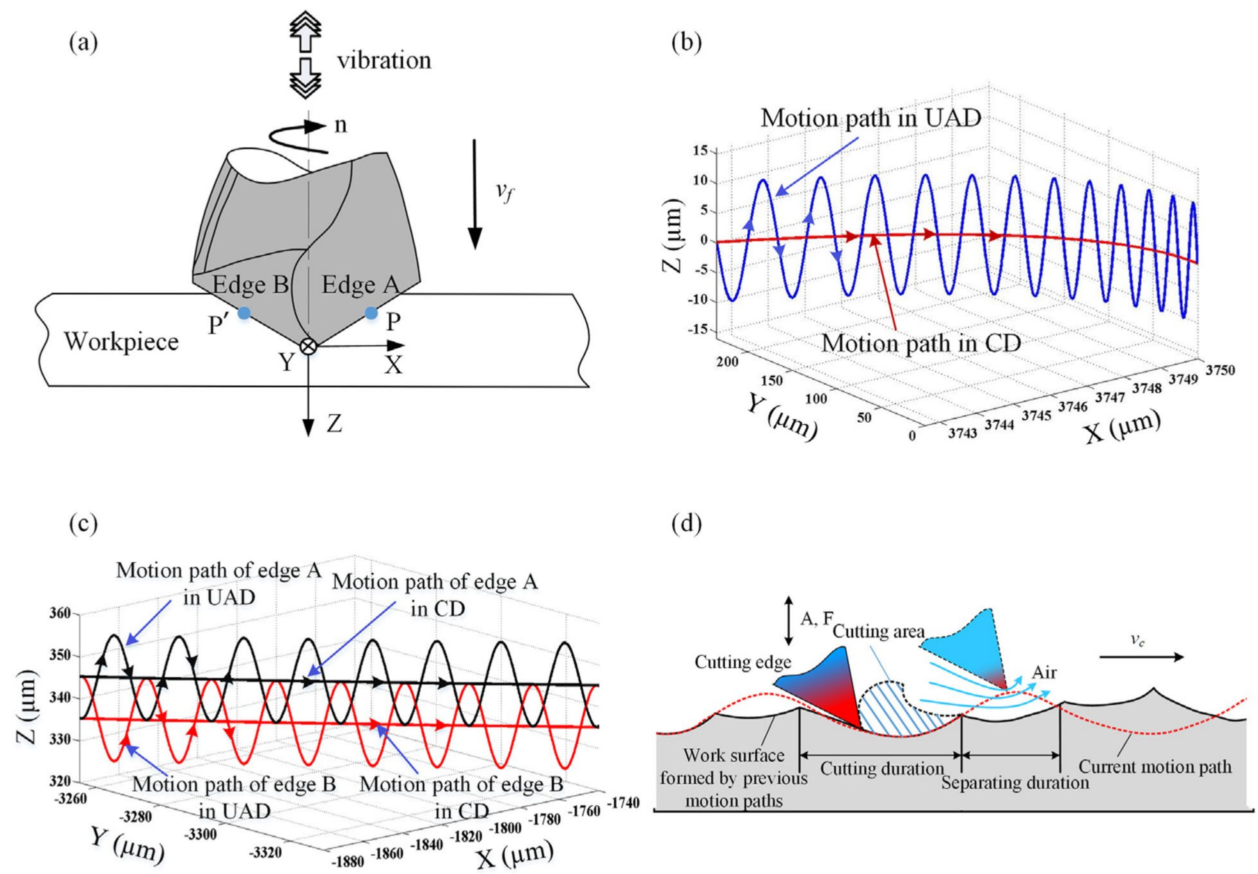

Figure 23 Different tool paths: **a** UAD process, **b** Moving locus of cutting edge for UAD and CD, **c** Moving locus of Edge A and Edge B for both UAD and CD, **d** The intermittent cutting mode in UAD [122]

force have an important impact on improving the accuracy of hole making, reducing machining damage and extending tool life [134–138].

Sakamoto et al. found that the faster the speed, the lower the drilling temperature when orbital drilling CFRP. This was because the high cutting speed increased the chip size and improved the material removal rate which accounted for the reduction of drilling temperature [139]. Liu et al. separately established the heat conduction models to learn about the temperature distribution in the workpiece when orbital drilling Ti6Al4V, CFRP and CFRP-Ti stacks. Based on the characteristics of helical milling, the models simplified the end edge and peripheral edge of the milling cutter into two heat sources, and then used different methods to solve the heat conduction model, such as Green's function, inverse heat conduction and integral transformation [140–142]. Figure 27 shows the temperature changes of different materials in orbital drilling.

6.4 Effect of Laser Drilling on Temperature

Laser drilling is a process of using a focused laser beam to melt or evaporate the material and remove the material along the depth of the hole (see Figure 28) [143, 144]. As a non-contact hole-making technology, laser drilling has great application potential. However, due to its high-temperature and high-radiation, it is easy to produce a heat-affected zone (HAZ), in which the structure and properties of the material change. Therefore, scholars have conducted a lot of research on how to solve the problem of heat-affected zone.

Bharatish et al. conducted laser drilling on ceramics and found that increasing the pulse frequency can effectively reduce the extent of the heat-affected zone [145]. For Ti6Al4V, because of the low thermal conductivity, the influence of laser power and pulse frequency on the heat-affected zone was negligible, but as the thickness of the workpiece increased, the range of the HAZ will also expand [146, 147]. What's more, Chatterjee et al. found that, when laser drilling Ti6Al4V, more heat was generated as the laser power increased, which allowed the heat

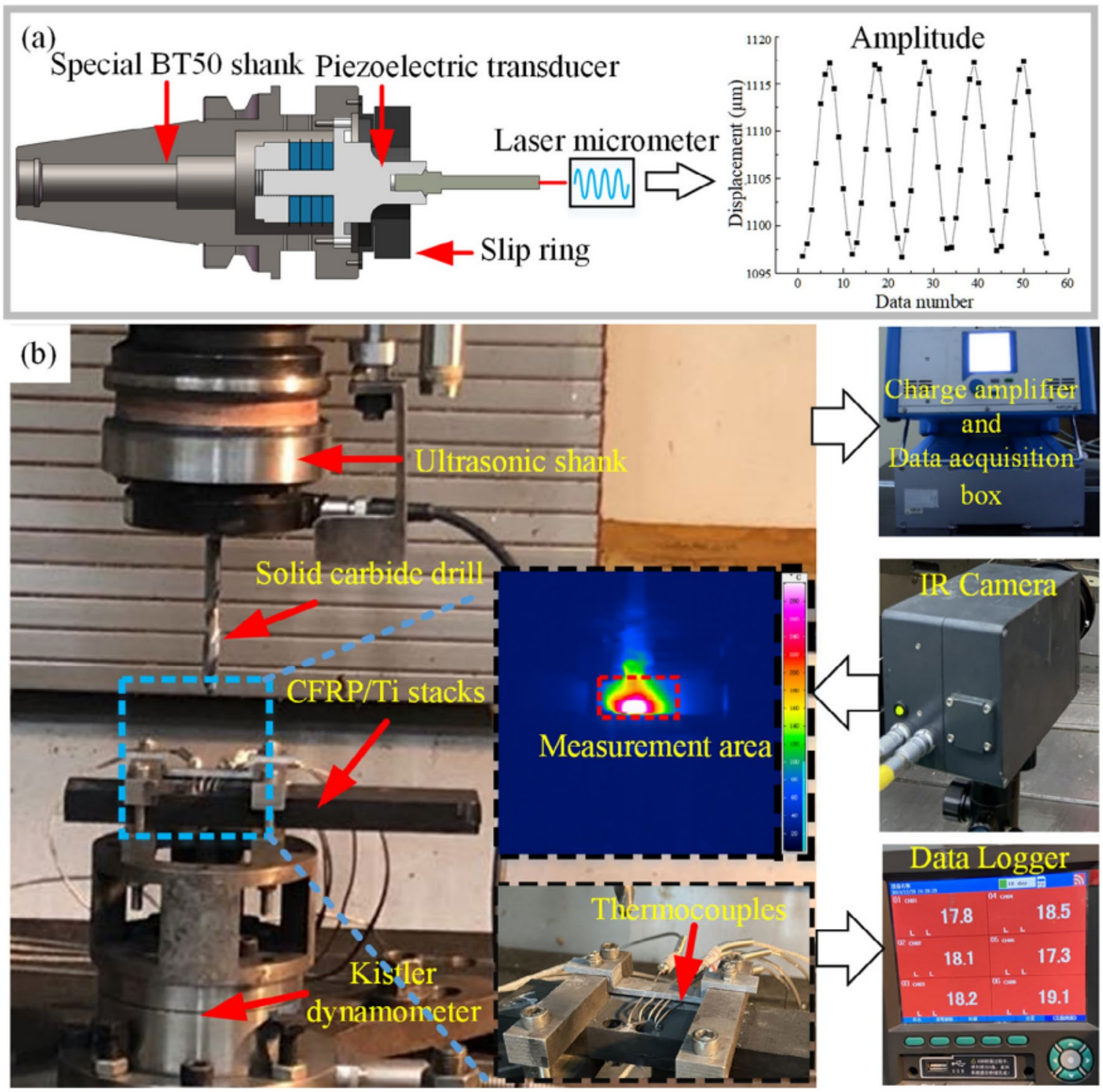

Figure 24 The system of UAD: **a** The details of ultrasonic shank and **b** Experimental setup [122]

to be effectively transferred to the bottom of the hole and alleviated the taper [148, 149]. Mishra's research showed that when laser drilling was performed on aluminum, the range of the heat-affected zone was proportional to the pulse frequency. This was because the larger the pulse frequency, the smaller the time interval between pulses, and thermal diffusion will occur in the radial direction, thus forming a larger heat-affected zone [150, 151]. Leone et al. studied the relationship between the HAZ and different process parameters such as average power, cutting speed, pulse frequency and pulse duration when laser drilling CFRP. He found that the range of the heat-affected zone between 170–1600 μm occurred at the center of the laminate in correspondence with unidirectional lamina and the heat-affected zone expansion was related to the spot overlap [152]. Weber et al. proposed a perpendicular heat flow model, which can derive the best pulse parameters according to the quality needs when laser drilling CFRP [153]. Ye et al. compared the influence of different laser drilling methods on the heat-affected zone, and found that the laser rotary cutting had a smaller heat-affected zone under the same parameters, but the surface flatness of the hole was slightly worse than the parallel filling and the cross filling [154]. Li et al. explored and compared the drilling defects including machined surface micro-defects, dimension error and

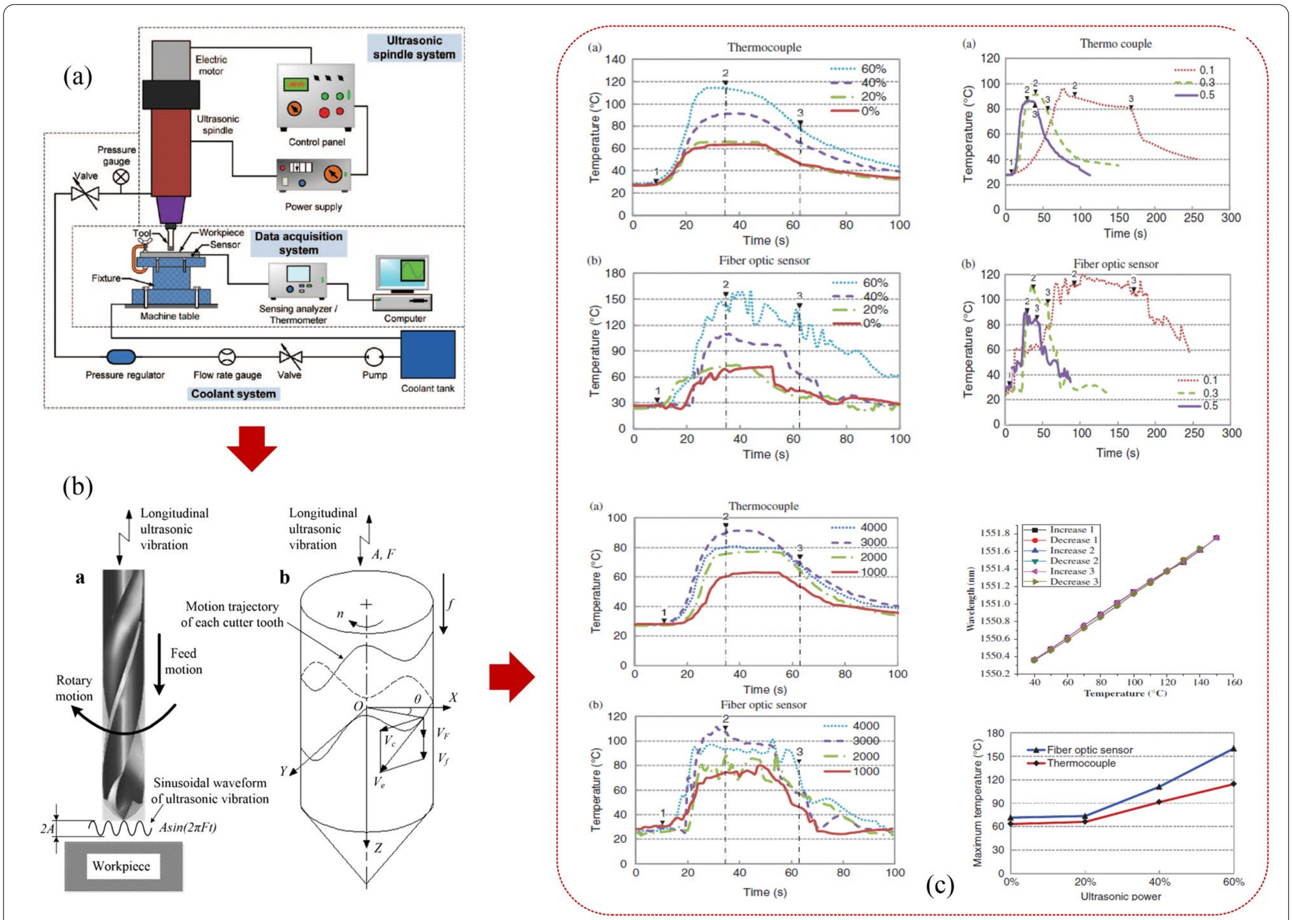

Figure 25 Results of UAD system: **a** schematic of experimental system, **b** schematic of UAD process and trajectory of each cutter tooth on the drill, **c** influence of different factors on ultrasonic vibration drilling temperature [119, 126]

heat-affected zone under spiral scanning mode and concentric scanning mode. The results showed that, compared with concentric scanning mode, spiral scanning mode reduced the size of HAZ by 33.42% and matrix recession (MR) by 24.83%, but the dimension errors were larger, including the circularity error and taper error, as shown in Figure 29 [155].

7 Controlling Methods for Drilling Temperature

During the drilling process, because it is in a semi-closed machining environment, the temperature rises sharply, which affects the tool life and the quality of the machined surface. Hence, a lot of efforts have been conducted to control the drilling temperature. In the traditional method, using a large amount of cutting fluid can indeed effectively reduce the drilling temperature and improve the drilling performance. However, large-scale use of cutting fluid is likely to cause environmental pollution and high costs such as material and manpower. In order to reduce the use of cutting fluid and lower the drilling temperature, scholars around the world have developed and applied different green cooling technologies, such as dry cutting, minimum quantity lubrication, cryogenic cooling and air cooling technology [156–159].

7.1 Minimum Quantity Lubrication (MQL)

The mechanism of MQL technology: when the atomized lubricating fluid is sprayed on the tool-chip and tool-workpiece interface, a lubricating oil film will be formed, thereby reducing the cutting heat generated by friction to achieve the cooling and lubrication of the contact interface. Due to the excellent performance of MQL technology in reducing tool wear, lowering drilling temperature and improving drilling quality, a large number of scholars have conducted research on this cooling technology [160–167].

Bhowmick et al. explored the machining characteristics of aluminum alloy drilling under dry cutting, H_2O-MQL and conventional flooded coolant, and the results showed that the cooling effect of H_2O-MQL drilling was

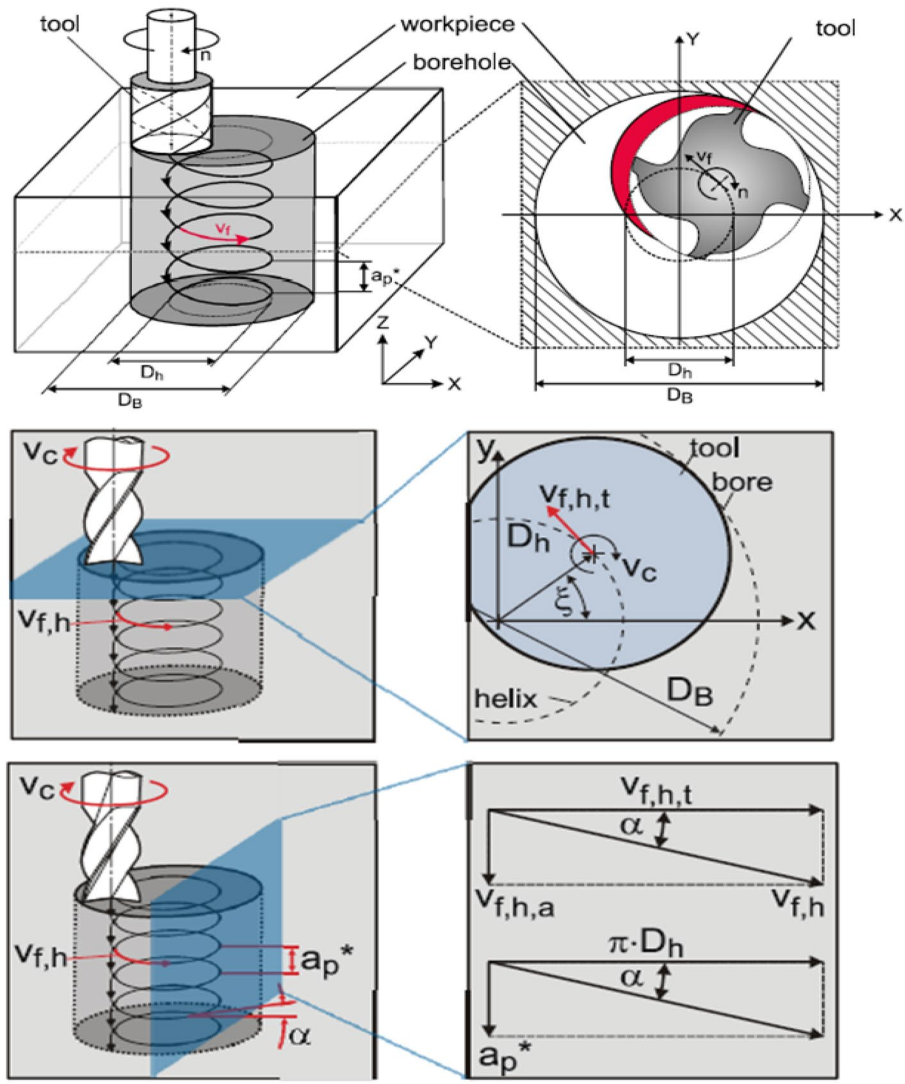

Figure 26 Moving locus and kinematics of orbital drilling [132].

equivalent to that of conventional flooded coolant and better than dry cutting. In another study, he used fatty acid-based MQL, which had a better cooling effect than H_2O-MQL [52, 168]. Rahim et al. also evaluated the effects of synthetic esters and palm oil-based MQL in drilling Ti6Al4V titanium alloys. The results showed that both synthetic esters and palm oil-based MQL greatly improved tool life. Furthermore, palm oil-based MQL had a superior lubricating ability which reduced the high friction. Additionally, the cooling capacity of palm oil-based MQL was good enough to reduce the drilling temperature [169].

Mathew's research showed that when drilling under the MQL environment, the drilling temperature was significantly lower compared with dry cutting (see Figure 30). What's more, due to the excess heat generated at the machining area was taken away by the cutting fluid supplied as the mist which can inhibit the built-up edge formation and effectively improve the surface roughness [170]. Murthy et al. evaluated the quality characteristics of dimensional deviation of hole diameter, chip thickness and energy consumption etc. when drilling aluminum alloy by using dry cutting, MQL and cutting fluid. The experimental results showed that compared with dry and wet machining, MQL reduced the dimensional deviation by 60% and 50% respectively. What's more, the chip thickness was also greatly reduced, thereby improving the chip removal and heat dissipation effect. Additionally, cutting energy consumption also reduced by 21.2% and 33% respectively [171].

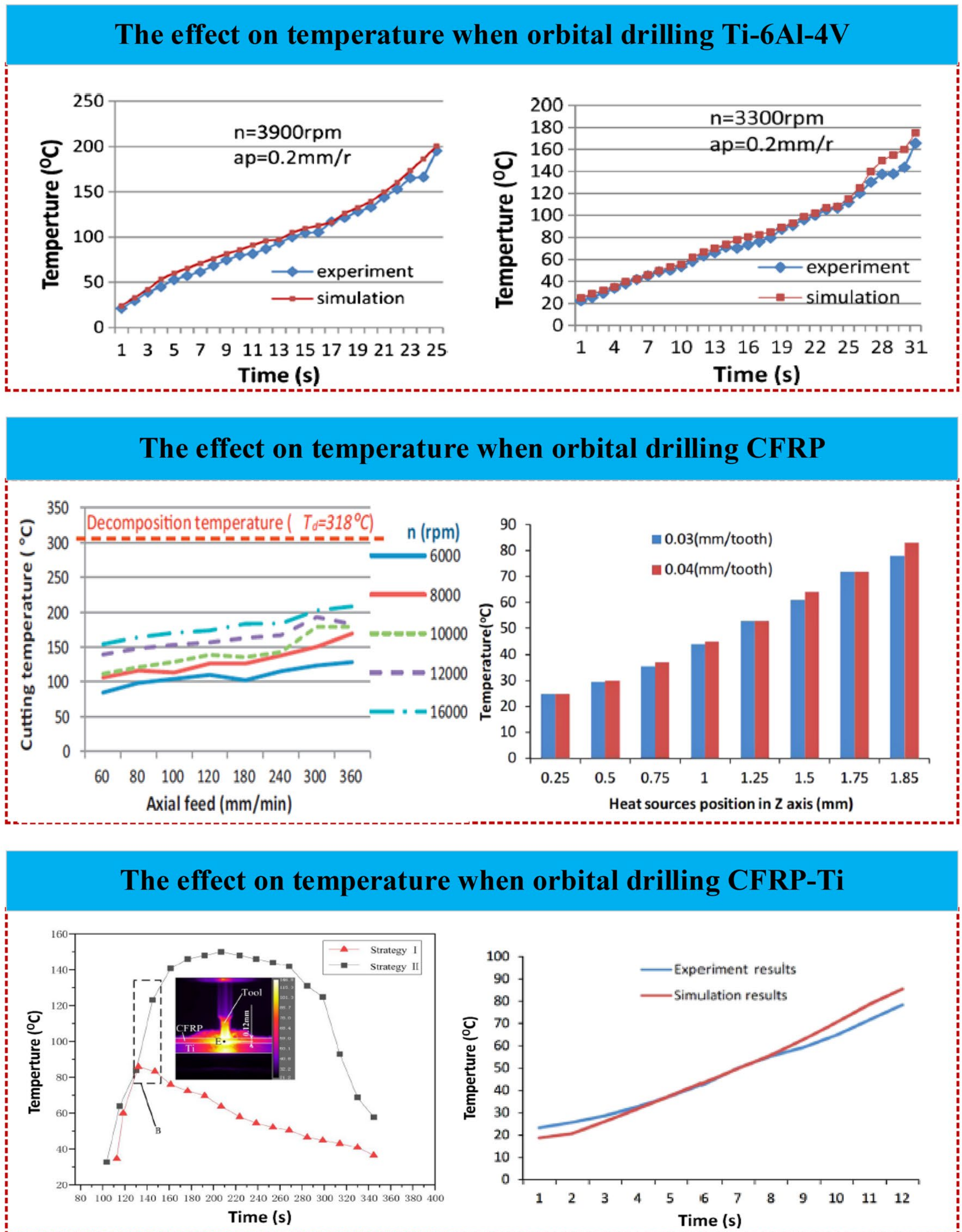

Figure 27 The effect on temperature when orbital drilling different materials [135, 137, 138, 141]

Kelly et al. found that it can effectively reduce thrust, torque and drilling temperature when using MQL for drilling. Furthermore, the research also pointed out that the alignment of the feed nozzle in relation to the tool, the pressure of the cutting fluid and the cutting fluid flow can be optimized to maximize the tool life [172].

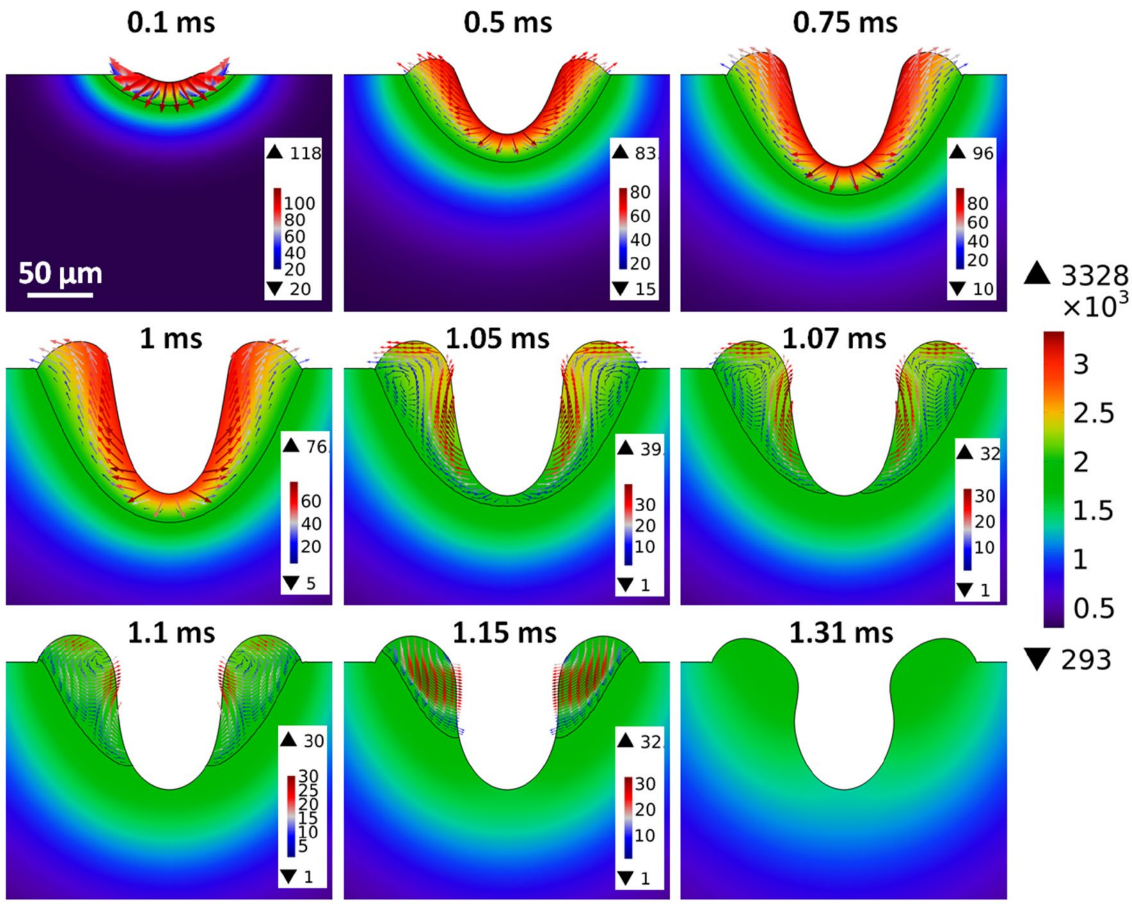

Figure 28 Evolution of melt pool shape for first pulse, temperature field and velocity field [144]

Zeilmann et al. found that, for the temperature distribution around the workpiece, the temperature measured using MQL applied internally through the drill (MQL int) was much smaller than the temperature measured by MQL applied with an external nozzle (MQL ext) [173]. Brinksmeier used MQL applied internally through the drill for drilling Aluminum CFPR/Ti6Al4V multi-layer materials and reached the same conclusion [174].

7.2 Air Cooling

Air cooling technology is a safe and environmentally friendly cooling technology [175–183]. Currently, the refrigeration methods used to develop cooling gas equipment mainly include vapor-compression refrigeration, liquid nitrogen evaporation refrigeration, vortex tube refrigeration and adiabatic expansion refrigeration [176]. The cooling system based on cold compressed air can effectively reduce the friction and heat in the cutting area, reduce tool wear during high-speed cutting, and can also play a good effect in drilling difficult-to-machine materials.

Domingo et al. found that the air cooling system can effectively reduce the energy consumption of the drilling process, and the air cooling system is suitable for high-speed processing by using vortex tubes to cool compressed air, and drills under different cutting parameters and ambient temperatures (−22 °C, 0 °C, 22 °C) [184]. Compared to the effects of dry cutting and air cooling on the cutting characteristics, Liu et al. found that the air cooling system can effectively reduce the drilling temperature and increase the service life of the tool. In addition, increasing the cutting speed and feed rate will weaken the cooling effect because of the increased heat-source area and heat flux and the maximum airflow was the most effective for reducing the drilling temperature [185].

Wu et al. explored the sustainable and high-throughput drilling of compacted graphite iron using dry cutting, through-the-drill compressed air and MQL respectively. It was found that the tool life under through-the-drill compressed air was longer than that of dry cutting and MQL. Through observation in a high-speed camera, it

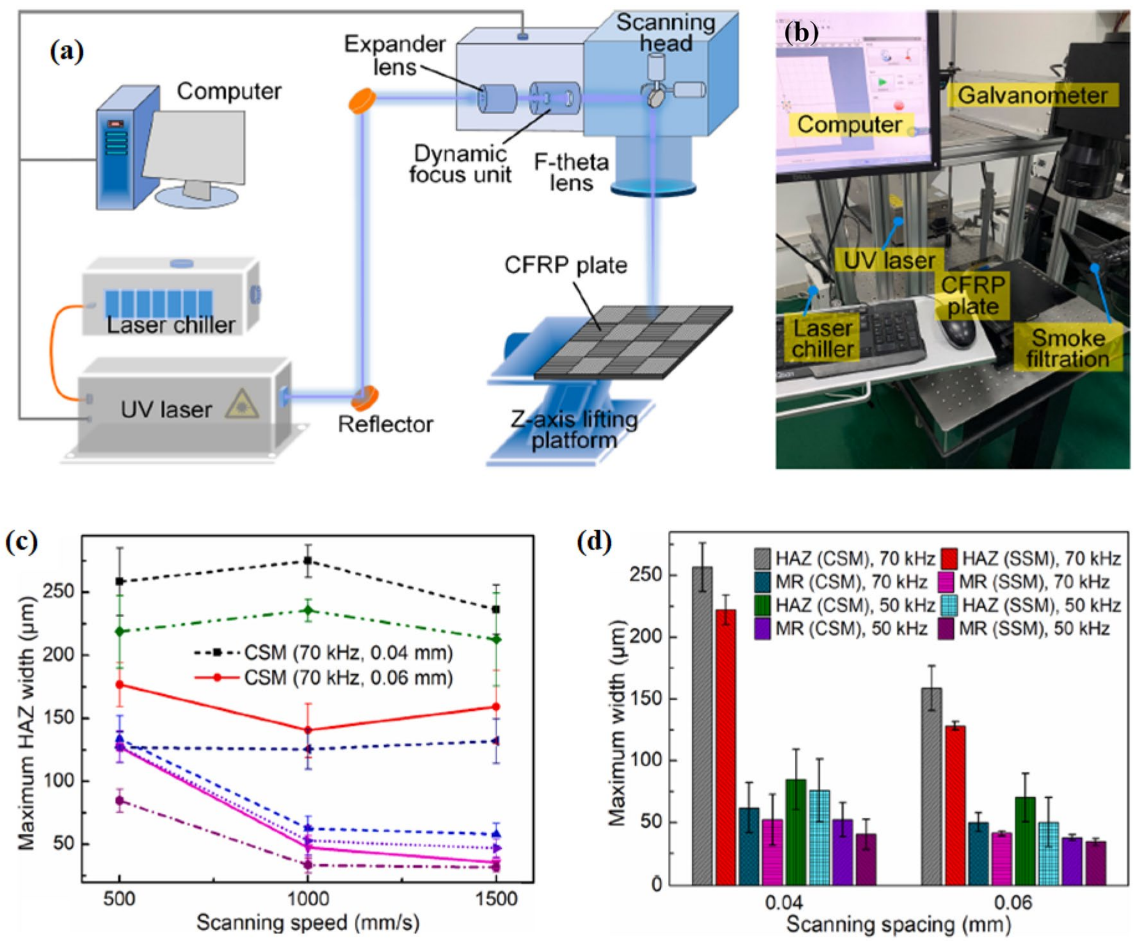

Figure 29 Effect of laser drilling on HAZ: **a** The schematic diagram of laser drilling system, **b** Experiment setup of laser drilling system, **c** Effect of scanning speed on HAZ under CSM and SSM, **d** Effect of scanning spacing on HAZ and MR under CSM and SSM [155]

was found that the chip removal speed under air cooling was faster than dry cutting and MQL, so it can effectively reduce tool wear, which was the main reason for the longer tool life under air cooling [186, 187]. But in another study, it was found that the tool life of drilling with MQL was twice as long as that under air-cooling conditions [188]. This may be related to the air flow rate in the air cooling system, workpiece materials and cutting fluid used by MQL.

Wang et al. proposed a reversed-air cooling technology for both enhancing the hole-exit support and reducing the drilling temperature. Its schematic diagram is shown in Figure 31, with the help of a vacuum cleaner, the air pressure in the cavity will reduce. Due to the pressure difference between the inside and outside of the cavity, an airflow will form from the outside to the inside which was opposite to the feed direction. The experimental results showed that when drilling CFRP, the reverse airflow can effectively reduce the drilling temperature and improve the hole-exit quality [189]. Fu et al. also proposed a reversed-air cooling system for purpose of achieving low-damage drilling of CFRP, as shown in Figure 32. Research showed that this system can effectively reduce the drilling temperature. In addition, due to the reverse air flow, an axial force opposite to the feed direction was generated, which strengthened the support of the material near the hole exit to a certain extent, and effectively suppressed the generation of burrs at the hole exit [190].

7.3 Cryogenic Cooling

Cryogenic cooling technology usually uses liquid nitrogen (LN_2) and liquid carbon dioxide (LCO_2) as coolants to lower the temperature, which is clean and environmentally friendly [191–195]. But different from other methods. It greatly reduces the temperature in the cutting zone and locally changes the mechanical properties of the workpiece surface and subsurface. A large number of studies have shown that cryogenic cooling technology

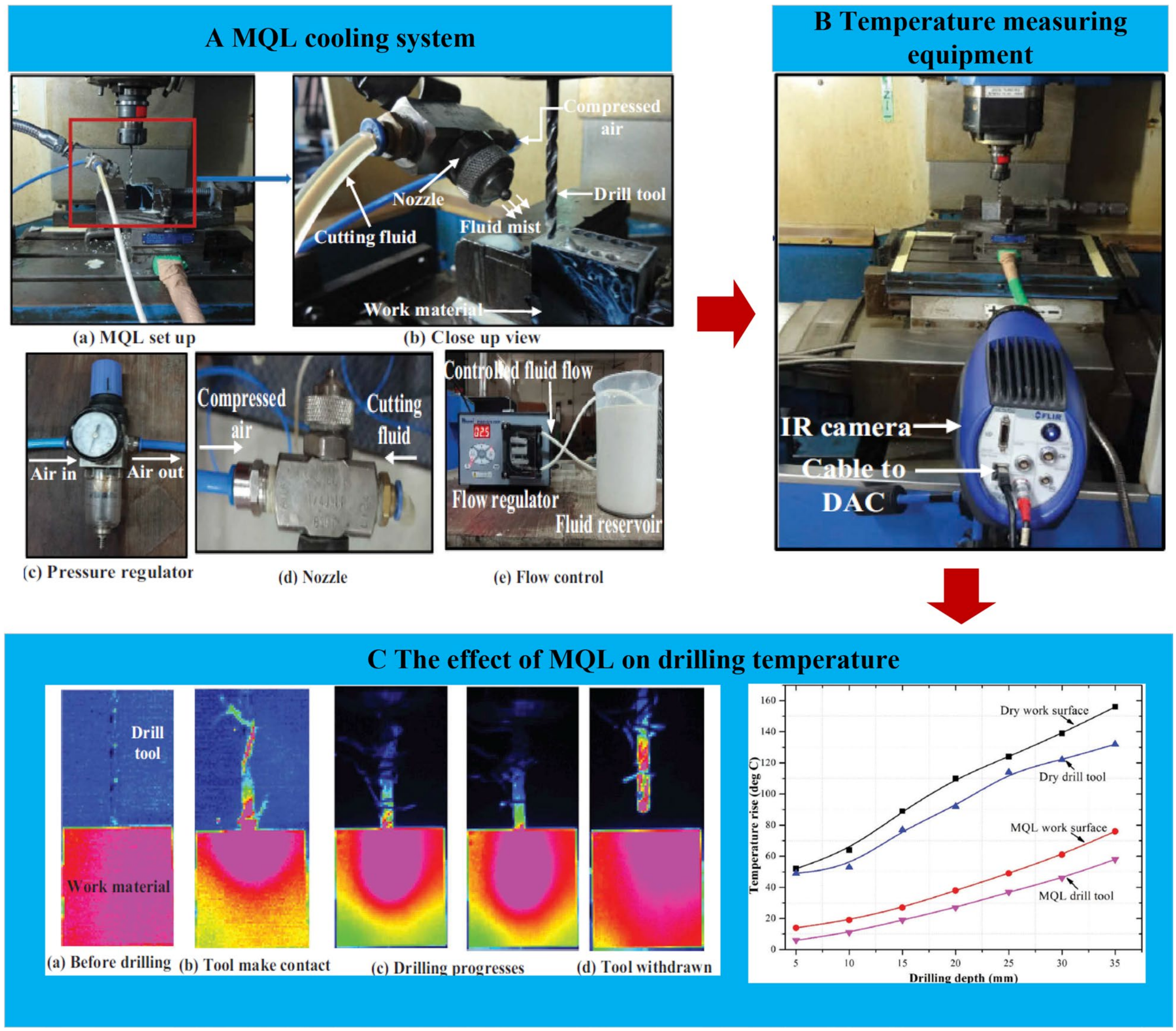

Figure 30 **A** is the MQL cooling system, **B** is temperature measuring equipment, **C** is the effect of MQL on drilling temperature [170]

can increase the hardness of the tool, reduce the coefficient of friction, and thereby extend the service life of the tool [196–202].

Perçin et al. presented a series of experimental investigations of the effects of cooling methods, such as dry cutting, flooded, MQL and cryogenic cooling when drilling Ti6Al4V. Research showed that increasing the spindle speed and reducing the feed rate can reduce the burr height. Among different cooling strategies, cryogenic cooling was the most effective method to reduce the burr height, and it performed better in terms of improving tool life [203]. Ahmed et al. performed a series of experiments when drilling Ti6Al4V in different cooling environments: cryogenic cooling and wet cooling environment. Based on TOPSIS method, they concluded that the use of liquid nitrogen for cryogenic cooling had longer tool life and better chip performance than the use of cutting fluids [204]. In another study of theirs, LN_2 cryogenic cooling and cutting fluid were used as coolants for drilling. The results proved that the use of LN_2 cryogenic cooling greatly reduced the drilling temperature, cutting force and torque, improved the surface roughness, and fully validated the superiority of LN_2 cryogenic cooling [205]. Barnes et al. observed that the tool cooled with liquid nitrogen had less exit delamination and overall internal damage when drilling CFRP, and the tool life was longer compared with dry cutting. However, the application of LN_2 cryogenic cooling didn't significantly

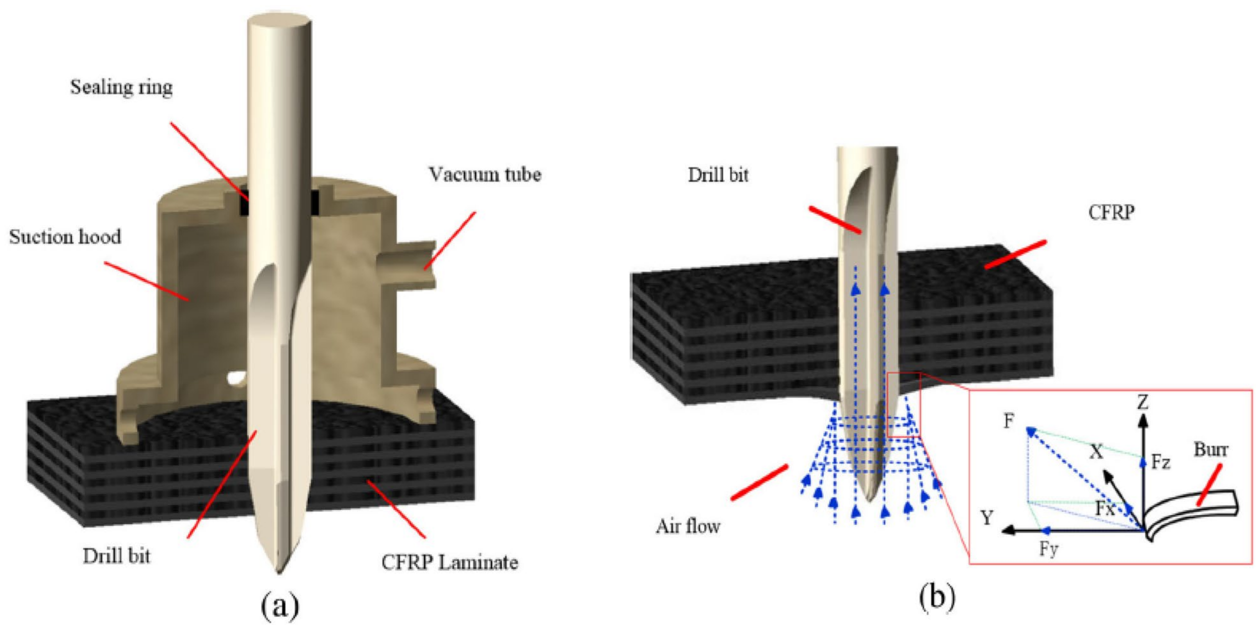

Figure 31 Schematic diagram of reverse-air cooling technology: **a** Setup, **b** Principle [189]

improve the drilling performance with respect to tool wear and cutting force [206]. When drilling Inconel 718, Uçak et al. found that the use of LN_2 cryogenic cooling can significantly reduce the drilling temperature (see Figure 33), while the hole quality and surface integrity were improved to a certain extent [207].

Liquid carbon dioxide (LCO_2) is also often applied in cryogenic cooling drilling. Under high pressure and low temperature conditions, carbon dioxide changes from gas to liquid, and it will absorb a lot of heat to reduce the drilling temperature when it evaporates. Nelson et al. drilled CFRP-Ti stacks under the cooling conditions of flooded and LCO_2 cryogenic cooling respectively. It was observed that the drilling temperature using LCO_2 cryogenic cooling was reduced by about 27% and energy consumption was reduced by 17%, what's more, a better surface finish and longer tool life can be obtained [208]. Sadik et al. conducted LCO_2 applied with the external nozzle and internally through the drill respectively. The research showed that LCO_2 applied internally through the drill significantly increased the tool life, and the effect of internal supply of CO_2 was expressed in two ways. On the one hand, it can effectively prevent the entry of external impurities. On the other hand, the internal supply of CO_2 can reduce built-up edge on the periphery insert [209].

8 Conclusions and Outlooks

In the past few decades, extensive efforts have been conducted on the drilling process and achieved a better understanding of drilling tool temperature. In this present paper, the recent advancements in drilling temperature have been reviewed with particular attention to theoretical analysis and thermal modeling, methods for temperature measuring, the effect of various factors (cutting parameters, tool geometries, and hole-making methods) on drilling temperature, and temperature controlling by different cooling methods. Based on the comprehensive review, some key conclusions on the current state-of-the-art and several possible prospects for future work can be drawn as follows.

(1) Based on the theoretical analysis, some significant thermal models during the drilling process have been conducted considering cutting parameters, tool geometries and tool wear. They also have been verified by numerical and experimental studies. However, relatively limited publications were found in the open literature dealing with the heat partition ratio among tools, workpieces and chips in the drilling. Further studies concerning thermal-mechanical coupling are necessary to establish the thermal model during the drilling process.
(2) The application of temperature measurement methods is relatively mature, but various methods have certain shortcomings. For instance, by using ther-

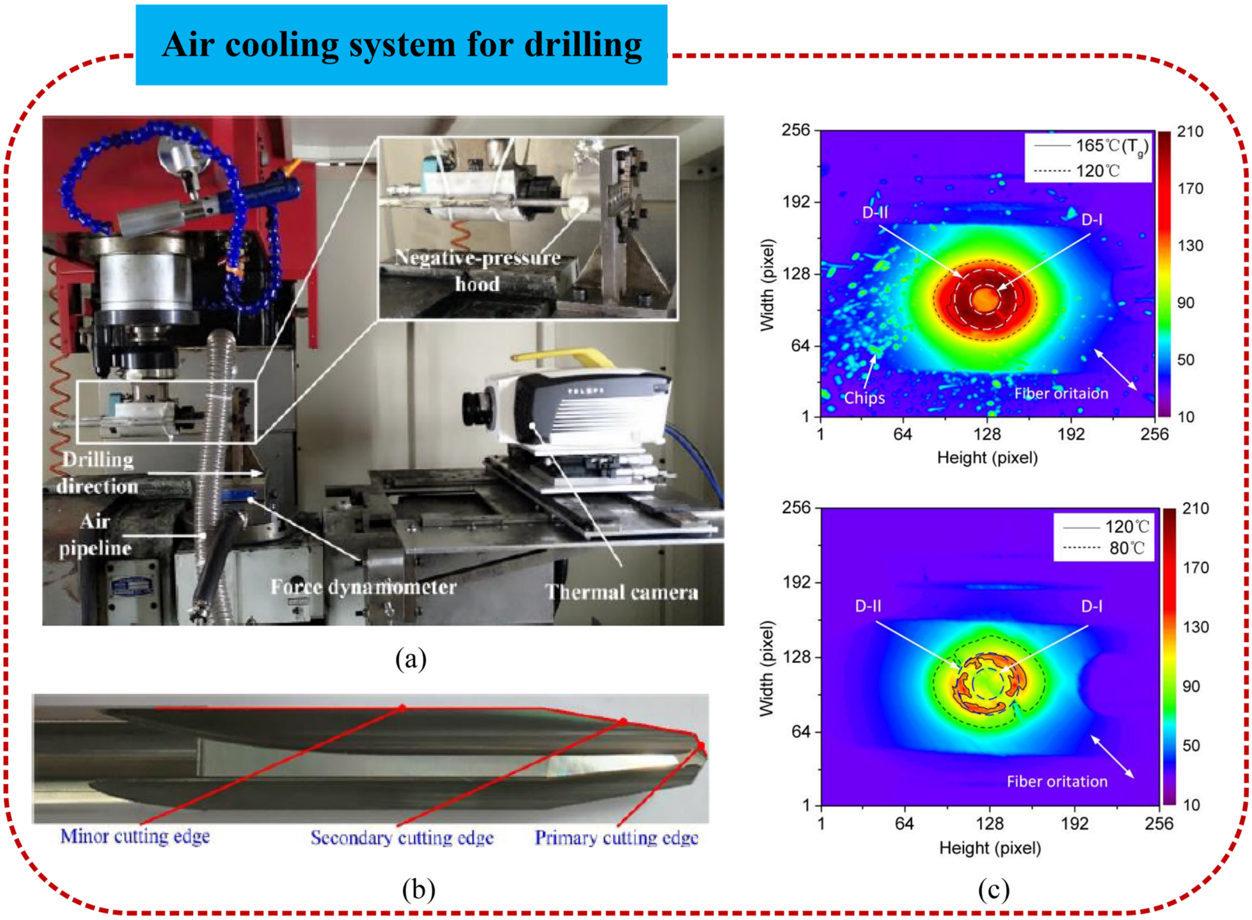

Figure 32 Air cooling system for drilling: **a** Experimental layout of drilling system, **b** Double point angle drill bit, **c** Distribution map of maximum temperatures at drill exit [190]

mocouples, they are pre-embedded in the workpiece or tool, so they cannot accurately measure the drilling temperature of the corresponding point; By using non-contact measurement methods, the temperature cannot be measured correctly as the drill penetrates the workpiece. Therefore, in actual experiments, it is more advocated to combine different measurement methods to reflect the temperature correctly during the drilling process.

(3) A lot of studies on the influence of cutting speed, feed rate and tool geometries on drilling temperature have been conducted. Judging from the results of various studies, the different workpiece materials, tool materials, and cooling methods used in the experiment may result in different results. The influence of these factors on drilling temperature is not a purely linear relationship. The selected tool material, workpiece material, cooling process, etc. are all important factors that affect the mechanism related to drilling temperature. Therefore, accurately grasping the correlation mechanism of cutting speed, feed rate, tool geometries and other factors on drilling temperature requires more in-depth and systematic exploration.

(4) In terms of hole-making methods, compared to conventional machining, the performances of LF-CAD and UAD in the field of advanced materials machining are proven to be superior owing to their various advantages. They can effectively improve the chip removal ability and hole quality, extend tool life and reduce the drilling tool temperature by using appropriate machining parameters (ultrasonic frequency, amplitude, etc). In addition, the orbital drilling is verified to be prone to generate discontinuous chips due to its special hole making mechanism, which can reduce the drilling temperature effectively. However, most of the existing studies are concerned with the 1D vibration drilling, the 2D UAD, especially on the drilling temperature during 2D UAD processing, is relatively limited.

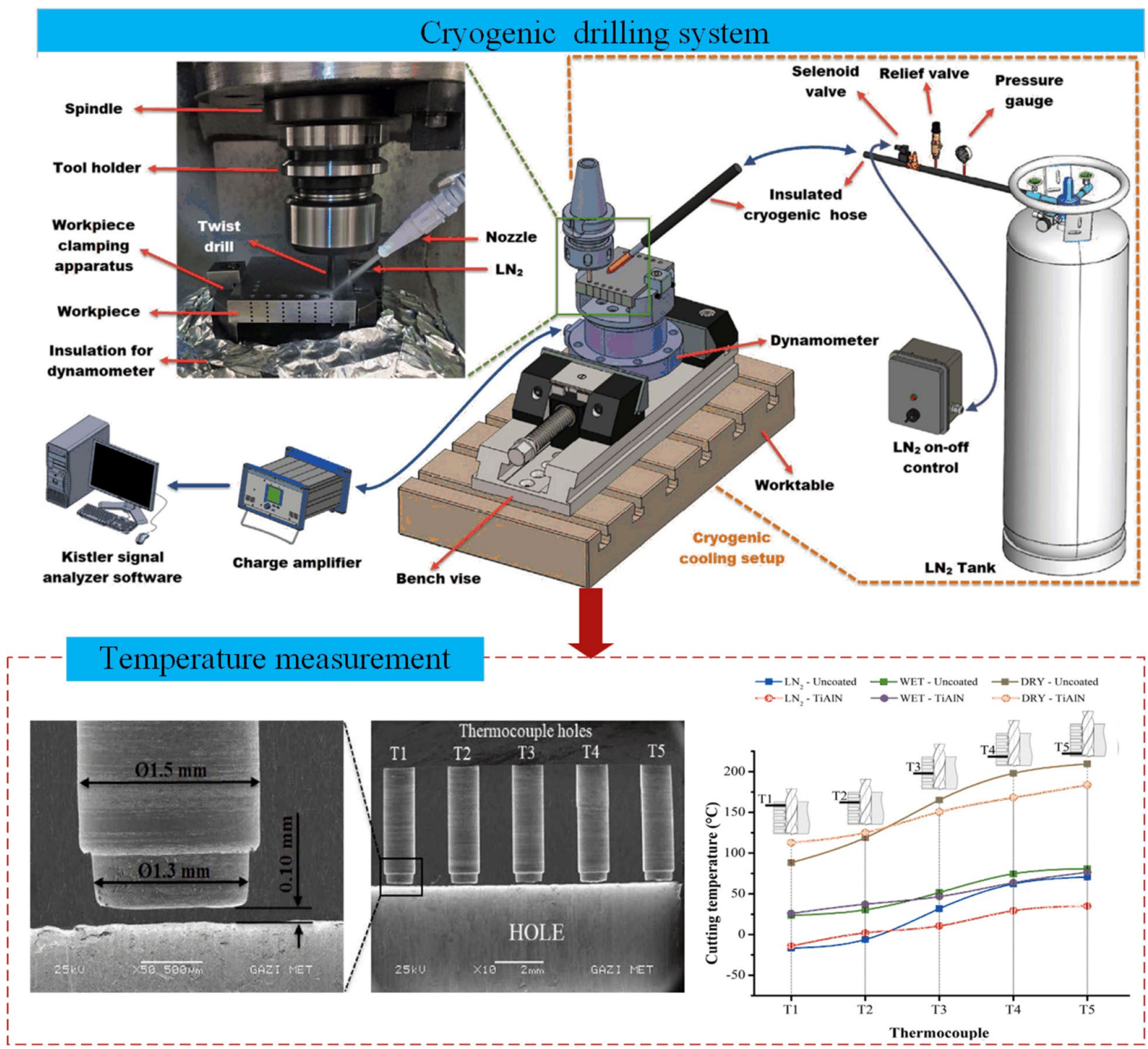

Figure 33 Cryogenic drilling system and drilling temperature values under different machining condition [207]

Consequently, in order to improve the machining efficiency and reduce the drilling tool temperature, novel intermittent drilling processes should be developed in the future.

(5) In terms of cooling methods, this present paper systematically outlines the existing cooling methods, which have a beneficial effect on reducing the drilling temperature and improving hole quality. Although the cooling ability of MQL is not as good as other cooling methods, it is more prominent in decreasing tool wear. Air cooling performs better in chip removal and heat dissipation, while the cryogenic cooling has the strongest cooling effect. However, more attention should be paid to brittle fracture of the material. In the development of new cooling methods, although a lot of research has been carried out and some beneficial results have been achieved, it is difficult to popularize and promote. The development and popularization of new cooling methods not only need to be effective in controlling drilling temperature and improving hole quality, but also should control manufacturing costs and be environmentally friendly, so there is still a long way to go.

Acknowledgements
Not applicable.

Author Contributions
ZJ carried out studies in reviews of drilling tool temperature. XH assisted with the structure and language of the manuscript. JS conducted proofreading and made some critical revisions. JF supervised every step of the entire work. All authors read and approved the final manuscript.

Authors' Information
Zhaoju Zhu, born in 1988, is currently a lecture at *School of Mechanical Engineering and Automation, Fuzhou University, China*. He received his PhD degree from *Shandong University*, *China*, in 2019. His research interests include advanced manufacturing and drilling laminates.
Xinhui Sun, born in 1996, is currently pursuing his master degree at *School of Mechanical Engineering and Automation, Fuzhou University, China*. His research interests include drilling temperature and advanced manufacturing.
Kai Guo, born in 1990, is currently an assistant professor at *School of Mechanical Engineering, Shandong University, China*. His research interests include advanced manufacturing and robotic machining.
Jie Sun, born in 1965, is currently a professor at *School of Mechanical Engineering, Shandong University*, *China*. His research interests include advanced manufacturing and 3D printing.
Jianfeng Li, born in 1963, is currently a professor at *School of Mechanical Engineering, Shandong University*, *China*. His research interests include advanced manufacturing and green manufacturing.

Funding
This work was supported by Natural and Science Foundation of China (Grant No. 52205455), Fujian Provincial Natural and Science Foundation (Grant No. 2021J01560) and Fujian Provincial Education and Scientific Research Foundation for Young Teachers (Grant No. JAT190006).

Data Availability
All data generated or analysed during this study are included in this published article. All data are fully available without restriction.

Competing Interests
The authors declare no competing financial interests.

Author Details
[1]School of Mechanical Engineering and Automation, Fuzhou University, Fuzhou 350116, China. [2]School of Mechanical Engineering, Shandong University, Jinan 250061, China.

Received: 1 November 2021 Revised: 27 September 2022 Accepted: 1 November 2022
Published online: 14 December 2022

References

[1] J Xu, C Li, J Dang, et al. A study on drilling high-strength CFRP laminates: Frictional Heat and Cutting Temperature. *Materials (Basel)*. 2018, 11(12): 2366–2378.
[2] Z Liu. *Finite element analysis and hole machining quality research on the drilling process of titanium alloy /CFRP Stack*. Tianjin: Tianjin University, 2016. (in Chinese)
[3] Z J Zhu. *Investigation on the tool temperature characteristics and key technologies for drilling aerospace heterostructure*. Jinan: Shandong University, 2019. (in Chinese)
[4] H X Yuan. Manufacturing technology of connecting hole in aircraft structures. *Aeronautical Manufacturing Technology*, 2007(1): 96–99. (in Chinese)
[5] A Nayebi, G Mauvoisin, H Vaghefpour. Modeling of twist drills wear by a temperature-dependent friction law. *Journal of Materials Processing Tech.*, 2008, 207(1): 98–106.
[6] M Nouari, G List, F Girot, et al. Experimental analysis and optimisation of tool wear in dry machining of aluminium alloys. *Wear*, 2003, 255(7): 1359–1368.
[7] J S Agapiou, D A Stephenson. Analytical and experimental studies of drill temperatures. *Journal of Engineering for Industry*, 1994, 116(1): 54–60.
[8] A R Watson. Drilling model for cutting lip and chisel edge and comparison of experimental and predicted results. I—initial cutting lip model. *International Journal of Machine Tool Design and Research,* 1985, 25(4): 347–365.
[9] F Ke, J Ni, D A Stephenson. Continuous chip formation in drilling. *International Journal of Machine Tools and Manufacture*, 2005, 45(15): 1652–1658.
[10] M Bono, J Ni. The effects of thermal distortions on the diameter and cylindricity of dry drilled holes. *International Journal of Machine Tools and Manufacture*, 2001, 41(15): 2261–2270.
[11] M Bono, J Ni. A model for predicting the heat flow into the workpiece in dry drilling. *Journal of Manufacturing Science and Engineering*, 2002, 124(4): 773–777.
[12] A Sadek, B Shi, M Meshreki, J Duquesne, et al. Prediction and control of drilling-induced damage in fibre-reinforced polymers using a new hybrid force and temperature modelling approach. *CIRP Annals - Manufacturing Technology*, 2015, 64(1): 89–92.
[13] K H Fuh, W C Chen, P W Liang. Temperature rise in twist drills with a finite element approach. *International Communications in Heat and Mass Transfer*, 1994, 21(3): 345–358.
[14] S Kalidas, S G Kapoor, R E DeVor. Influence of thermal effects on hole quality in dry drilling, part 1: a thermal model of workpiece temperatures. *Journal of Manufacturing Science and Engineering*, 2002, 124(2): 258–266.
[15] S Kalidas, R E DeVor, S G Kapoor. Experimental investigation of the effect of drill coatings on hole quality under dry and wet drilling conditions. *Surface and Coatings Technology*, 2001, 148(2–3): 117–128.
[16] A T Kuzu, K R Berenji, B C Ekim, et al. The thermal modeling of deep-hole drilling process under MQL condition. *Journal of Manufacturing Processes*, 2017, 29: 194–203.
[17] J Wu, R D Han. A new approach to predicting the maximum temperature in dry drilling based on a finite element model. *Journal of Manufacturing Processes*, 2009, 11(1): 19–30.
[18] B Camille, P Thomas, L Yann. Development of a multi-scale and coupled cutting model for the drilling of Ti-6Al-4V. *CIRP Journal of Manufacturing Science and Technology*, 2021, 35: 526–540.
[19] G P Zhu, Y J Bao, H Gao. Research on the drilling temperature field model of the unidirectional carbon fiber epoxy composites. *Advanced Materials Research*, 2012, 565: 478–483.
[20] F J Wang, J Yin, J W Ma, et al. Heat partition in dry orthogonal cutting of unidirectional CFRP composite laminates. *Composite Structures*, 2018,197: 28–38.
[21] H S Patne, A Kumar, S Karagadde, et al. Modeling of temperature distribution in drilling of titanium. *International Journal of Mechanical Sciences*, 2017, 133: 598–610.
[22] E M Berliner, V P Krainov. Analytic calculations of the temperature field and heat flows on the tool surface in metal cutting due to sliding friction. *Wear*, 1991, 143(2): 379–395.
[23] J Díaz-Álvarez, A Olmedo, C Santiuste, et al. Theoretical estimation of thermal effects in drilling of woven carbon fiber composite. *Materials*, 2014, 7(6): 4442–4454.
[24] A O Schmidt. Distribution of heat generated in drilling. *Trans ASME*, 1949, 71: 245–252.
[25] L Reissig, R Völkl, M J Mills, et al. Investigation of near surface structure in order to determine process-temperatures during different machining processes of Ti6Al4V. *Scripta Materialia*, 2004, 50(1): 121–126.
[26] B Mills, T D Mottishaw, A W J Chisholm. The application of scanning electron microscopy to the study of temperatures and temperature distributions in M2 high speed steel twist drills. *CIRP Annals*, 1981, 30(1): 15–20.
[27] P K Wright. Metallographic methods of determining temperature gradients in cutting tools. *Journal of the Iron and Steel Institute*, 1973, 211: 364–388.
[28] S Vaidyanathan. Predicting tool-life equation from temperature measurement. *International Journal of Production Research*,1970, 8(1): 51–57.
[29] C E Leshock, Y C Shin. Investigation on cutting temperature in turning by a tool-work thermocouple technique. *Journal of Manufacturing Science and Engineering*, 1997, 119(4A): 502–508.

[30] D A Stephenson. Tool-work thermocouple temperature measurements—Theory and implementation issues. *Journal of Engineering for Industry*,1993,115(4): 432–437.
[31] N Laraqi. Phénomène de constriction thermique dans les contacts glissants. *International Journal of Heat and Mass Transfer*, 1996, 39(17): 3717–3724.
[32] E Bağci, B Ozcelik. Influence of cutting parameters on drill bit temperature in dry drilling of AISI 1040 steel material using statistical analysis. *Industrial Lubrication and Tribology*, 2007, 59(4): 186–193.
[33] K Weinert, C Kempmann. Cutting temperatures and their effects on the machining behaviour in drilling reinforced plastic composites. *Advanced Engineering Materials*, 2004, 6(8): 684–689.
[34] J Xu, C Li, M Chen, et al. On the analysis of temperatures, surface morphologies and tool wear in drilling CFRP/Ti6Al4V stacks under different cutting sequence strategies. *Composite Structures*, 2020, 234: 111708.
[35] M F DeVries, U K Saxena, S M Wu. Temperature distributions in drilling. *Journal of Engineering for Industry*,1968, 90(2): 231–238.
[36] J Battaglia, A Kusiak. Estimation of heat fluxes during high-speed drilling. *The International Journal of Advanced Manufacturing Technology*, 2005, 26(7–8): 750–758.
[37] R Li, A J Shih. Tool temperature in titanium drilling. *Journal of Manufacturing Science and Engineering*, 2007, 129(4): 740–749.
[38] R Li, A J Shih. Spiral point drill temperature and stress in high-throughput drilling of titanium. *International Journal of Machine Tools and Manufacture*, 2007, 47(12): 2005–2017.
[39] J L Merino-Pérez, R Royer, S Ayvar-Soberanis, et al. On the temperatures developed in CFRP drilling using uncoated WC-Co tools Part I: Workpiece constituents, cutting speed and heat dissipation. *Composite Structures*, 2015, 123: 161–168.
[40] L Cardoso, R T Coelho, C H Lauro. Contribution to dynamic characteristics of the cutting temperature in the drilling process considering one dimension heat flow. *Applied Thermal Engineering*, 2011, 31(17): 3806–3813.
[41] M Bono, J Ni. A method for measuring the temperature distribution along the cutting edges of a drill. *Journal of Manufacturing Science and Engineering*, 2002, 124(4): 921–926.
[42] M Bono, J Ni. The location of the maximum temperature on the cutting edges of a drill. *International Journal of Machine Tools and Manufacture*, 2005, 46(7): 901–907.
[43] T Ueda, K Yamada, T Sugita. Measurement of grinding temperature of ceramics using infrared radiation pyrometer with optical fiber. *Journal of Engineering for Industry*, 1992, 114(3): 317–322.
[44] G Yang, J Z Hou, W Zhou, et al. Non-contact temperature measurement by infrared pyrometer in high speed milling. *Applied Mechanics and Materials*, 2014, 668: 969–972.
[45] T Ueda, M Sato, A Hosokawa, et al. Development of infrared radiation pyrometer with optical fibers—Two-color pyrometer with non-contact fiber coupler. *CIRP Annals*, 2008, 57(1): 69–72.
[46] M Okada, N Asakawa, Y Fujita, et al. Cutting characteristics of twist drill having cutting edges for drilling and reaming. *Journal of Mechanical Science and Technology*, 2014, 28(5): 1951–1959.
[47] T Beno, U Hulling. Measurement of cutting edge temperature in drilling. *Procedia CIRP*, 2012, 3: 531–536.
[48] S P F C Jaspers, J H Dautzenberg, D A Taminiau. Temperature measurement in orthogonal metal cutting. *The International Journal of Advanced Manufacturing Technology*, 1998, 14(1): 7–12.
[49] P Kwon, T Schiemann, R Kountanya. An inverse estimation scheme to measure steady-state tool–chip interface temperatures using an infrared camera. *International Journal of Machine Tools and Manufacture*, 2001, 41(7): 1015–1030.
[50] J Chen, Q L An, F Zou, et al. Analysis of low-frequency vibration-assisted bone drilling in reducing thermal injury. *Materials and Manufacturing Processes*, 2021, 36(1): 27–38.
[51] E Belotserkovsky, A Zur, A Katzir. Nonuniform temperature distribution monitoring with an IR fiber-optic radiometer. *Applied Optics*, 1994, 33(1): 64–67.
[52] S Bhowmick, J L Michael, T A Ahmet. Dry and minimum quantity lubrication drilling of cast magnesium alloy (AM60). *International Journal of Machine Tools and Manufacture*, 2010, 50(5): 444–457.
[53] A Taskesen, K Kutukde. Non-contact measurement and multi-objective analysis of drilling temperature when drilling B4C reinforced aluminum composites. *Transactions of Nonferrous Metals Society of China*, 2015, 25(1): 271–283.
[54] S Luka, K Peter, P Franci. The effects of liquid-CO_2 cooling, MQL and cutting parameters on drilling performance. *CIRP Annals - Manufacturing Technology*, 2021, 70(1): 79–82.
[55] E Oezkaya, M Bücker, S Strodick, et al. A thermomechanical analysis leading to a novel flank face design providing longer tool lives for tools used in the drilling of Inconel 718. *The International Journal of Advanced Manufacturing Technology*, 2019, 102(9–12): 2977–2992.
[56] J Dörr, T Mertens, G Engering, et al. 'In-situ'temperature measurement to determine the machining potential of different tool coatings. *Surface and Coatings Technology*, 2003, 174: 389–392.
[57] U A Khashaba, M S AbdElwahed, M A Eltaher, et al. Thermo-mechanical and delamination properties in drilling gfrp composites by various drill angles. *Polymers*, 2021, 13(11): 1884–1906.
[58] Y M Quan, L H Sun. Experimental investigation on drilling temperature of composites. *International Journal of Machining and Machinability of Materials*, 2008, 3(3–4): 356–363.
[59] R Çakıroğlu, A Acır. Optimization of cutting parameters on drill bit temperature in drilling by Taguchi method. *Measurement*, 2013, 46(9): 3525–3531.
[60] G Le Coz, M Marinescu, A Devillez, et al. Measuring temperature of rotating cutting tools: Application to MQL drilling and dry milling of aerospace alloys. *Applied Thermal Engineering*, 2011, 36: 434–441.
[61] B Ozcelik, E Bagci. Experimental and numerical studies on the determination of twist drill temperature in dry drilling: A new approach. *Materials & Design*, 2006, 27(10): 920–927.
[62] E Bağci, B Ozcelik. Investigation of the effect of drilling conditions on the twist drill temperature during step-by-step and continuous dry drilling. *Materials & Design*, 2006, 27(6): 446–454.
[63] T Ueda, R Nozaki, A Hosokawa. Temperature measurement of cutting edge in drilling -effect of oil mist. *CIRP Annals - Manufacturing Technology*, 2007, 56(1): 93–96.
[64] J Wu, R D Han. A new approach to predicting the maximum temperature in dry drilling based on a finite element model. *Journal of Manufacturing Processes*, 2009, 11(1): 19–30.
[65] N Joy, S Prakash, A Krishnamoorthy, et al. Experimental investigation and analysis of drilling in Grade 5 Titanium alloy (Ti-6Al-4V). *Materials Today: Proceedings*, 2020, 21: 335–339.
[66] A K Parida. Simulation and experimental investigation of drilling of Ti-6Al-4V alloy. *International Journal of Lightweight Materials and Manufacture*, 2018, 1(3): 197–205.
[67] R Bertolini, E Savio, A Ghiotti, et al. The effect of cryogenic cooling and drill bit on the hole quality when drilling magnesium-based fiber metal laminates. *Procedia Manufacturing*, 2021, 53: 118–127.
[68] G S Samy, S T Kumaran. Measurement and analysis of temperature, thrust force and surface roughness in drilling of AA (6351)-B4C composite. *Measurement*, 2017, 103: 1–9.
[69] E Ünal. Temperature and thrust force analysis on drilling of glass fiber reinforced plastics. *Thermal Science*, 2019, 23(1): 347–352.
[70] J Xu, C Li, M El Mansori, et al. Study on the frictional heat at tool-work interface when drilling CFRP composites. *Procedia Manufacturing*, 2018, 26: 415–423.
[71] R Chen, S J Li, C P Li, et al. Influence of fiber direction and processing parameters on drilling temperature of CFRP. *Journal of Mechanical Science and Technology*, 2021, 35(4): 1663–1669.
[72] R Zitoune, N Cadorin, F Collombet, et al. Temperature and wear analysis in function of the cutting tool coating when drilling of composite structure: In situ measurement by optical fiber. *Wear*, 2017, 376: 1849–1858.
[73] Q L An, J Q Dang, J L Li, et al. Investigation on the cutting responses of CFRP/Ti stacks: With special emphasis on the effects of drilling sequences. *Composite Structures*, 2020, 253: 122794.
[74] W C Chen. Some experimental investigations in the drilling of carbon fiber-reinforced plastic (CFRP) composite laminates. *International Journal of Machine Tools and Manufacture*, 1997, 37(8): 1097–1108.
[75] S Rawat, H Attia. Wear mechanisms and tool life management of WC–Co drills during dry high speed drilling of woven carbon fibre composites. *Wear*, 2009, 267(5): 1022–1030.

[76] L Sorrentino, S Turchetta, C Bellini. In process monitoring of cutting temperature during the drilling of FRP laminate. *Composite Structures*, 2017, 168: 549–561.
[77] Z J Zhu, K Guo, J Sun, et al. Evaluation of novel tool geometries in dry drilling aluminium 2024-T351/titanium Ti6Al4V stack. *Journal of Materials Processing Tech.*, 2018, 259: 270–281.
[78] Z Y Jia, Y Bai, F J Wang, et al. Effect of drill flute direction on delamination at the exit in drilling carbon fiber reinforced plastic. *Polymer Composites*, 2019, 40(S2): 1434–1440.
[79] Z Y Jia, R Fu, B Niu, et al. Novel drill structure for damage reduction in drilling CFRP composites. *International Journal of Machine Tools and Manufacture*, 2016, 110: 55–65.
[80] F J Wang, B Y Zhang, Z Y Jia, et al. Structural optimization method of multitooth cutter for surface damages suppression in edge trimming of carbon fiber reinforced plastics. *Journal of Manufacturing Processes*, 2019, 46: 204–213.
[81] K Liu, J F Li, J Sun, et al. Investigation on chip morphology and properties in drilling aluminum and titanium stack with double cone drill. *The International Journal of Advanced Manufacturing Technology*, 2018, 94(5): 1947–1956.
[82] W Liang, J K Xu, W F Ren, et al. Study on the influence of tool point angle on ultrasonic vibration–assisted drilling of titanium alloy. *The International Journal of Advanced Manufacturing Technology*, 2019, 105(1): 1069–1082.
[83] M SenthilKumar, A Prabukarthi, V Krishnaraj. Study on tool wear and chip formation during drilling carbon fiber reinforced polymer (CFRP)/titanium alloy (Ti6Al4V) stacks. *Procedia Engineering*, 2013, 64: 582–592.
[84] Q W YAO, Y Chen, H J Yang, et al. Effect of drill geometry parameters on axial force and drilling temperature of low frequency vibration drilling CFRP/titanium alloy stack Materials. *Tool Engineering*, 2019, 53(3): 28–32. (in Chinese)
[85] H Wang. *Study on drills of vibration assisted drilling CFRP/TC4 Stacks*. Nanjing: Nanjing University of Aeronautics and Astronautics, 2018. (in Chinese)
[86] J Liu. *Optimization of drilling processing parameters for Ti-CFRP-Ti laminated material*. Qinhuangdao: Yanshan University, 2019. (in Chinese)
[87] M F DeVries, S M Wu. Evaluation of the effects of design variables on drill temperature responses. *Journal of Engineering for Industry*,1970, 92(3): 699–705.
[88] N Sugita, M Oshima, K Kimura, et al. Novel drill bit with characteristic web shape for high efficiency and accuracy. *CIRP Annals - Manufacturing Technology*, 2018, 67(1): 69–72.
[89] Q L An, W W Ming, X J Cai, et al. Study on the cutting mechanics characteristics of high-strength UD-CFRP laminates based on orthogonal cutting method. *Composite Structures*, 2015, 131: 374–383 .
[90] J Ahmad. *Machining of polymer composites*. New York: Springer, 2009.
[91] L M Shu, S H Li, Z L Fang, et al. Study on dedicated drill bit design for carbon fiber reinforced polymer drilling with improved cutting mechanism. *Composites Part A: Applied Science and Manufacturing*, 2021, 142: 106259.
[92] N Sugita, L M Shu, K Kimura, et al. Dedicated drill design for reduction in burr and delamination during the drilling of composite materials. *CIRP Annals - Manufacturing Technology*, 2019, 68(1): 89–92.
[93] W C Chen. Effect of the cross-sectional shape design of a drill body on drill temperature distributions. *International Communications in Heat and Mass Transfer*, 1996, 23(3): 355–366.
[94] D Müller, B Kirsch, J C Aurich. The influence of structured flank faces on cooling performance when drilling. *Procedia CIRP,* 2019, 82: 415–420.
[95] K Pang, D Z Wang. Study on the performances of the drilling process of nickel-based superalloy Inconel 718 with differently micro-textured drilling tools. *International Journal of Mechanical Sciences*, 2020, 180: 105658.
[96] K K Wika, A R C. Sharman, D Goulbourne, et al. Impact of number of flutes and helix angle on tool performance and hole quality in drilling composite/titanium stacks. SAE, 2011-01-2744, 2011.
[97] T Paulsen, N Guba, J Sölter, et al. Influence of the workpiece material on the cutting performance in low frequency vibration assisted drilling. *CIRP Journal of Manufacturing Science and Technology*, 2020, 31: 140–152.
[98] Z D Li, J W Tian, F Jiao. Research and development progress of machine type low-frequency vibration motion technology. *Tool Engineering*, 2018, 52(1): 7–10. (in Chinese)
[99] S M Li, D Y Zhang, C J Liu, et al. Exit burr height mechanistic modeling and experimental validation for low-frequency vibration-assisted drilling of aluminum 7075-T6 alloy. *Journal of Manufacturing Processes*, 2020, 56: 350–361.
[100] S Marco, B Rachele, G Andrea, et al. Tool wear analysis in high-frequency vibration-assisted drilling of additive manufactured Ti6Al4V alloy. *Wear*, 2021: 203814.
[101] L Wei, D Z Wang. Comparative study on drilling effect between conventional drilling and ultrasonic-assisted drilling of Ti-6Al-4V/Al2024-T351 laminated material. *The International Journal of Advanced Manufacturing Technology*, 2019, 103(1–4): 141–152.
[102] B J Huo, B Zhao, L Yin, et al. Effect of double-excitation ultrasonic elliptical vibration turning trajectory on surface morphology. *The International Journal of Advanced Manufacturing Technology*, 2021, 113(5): 1401–1414.
[103] P A Rey, J LeDref, J Senatore, et al. Modelling of cutting forces in orbital drilling of titanium alloy Ti–6Al–4V. *International Journal of Machine Tools and Manufacture*, 2016, 106: 75–88.
[104] R B D Pereira, L C Brandão, A P de Paiva, et al. A review of helical milling process. *International Journal of Machine Tools and Manufacture*, 2017, 120: 27–48.
[105] H Yagishita, Y Morita. Effect of phase transformation upon hole making accuracy of Ti6Al4V by orbital drilling. *Procedia Manufacturing*, 2018, 26: 152–163.
[106] G D Gautam, A K Pandey. Pulsed Nd: YAG laser beam drilling: A review. *Optics and Laser Technology*, 2018, 100: 183–215.
[107] D Abidou, A A D Sarhan, N Yusoff, et al. Numerical simulation of metal removal in laser drilling using meshless local Petrov–Galerkin collocation method. *Applied Mathematical Modelling*, 2018, 56: 239–253.
[108] S Sharma, V Mandal, S A Ramakrishna, et al. Numerical simulation of melt hydrodynamics induced hole blockage in Quasi-CW fiber laser micro-drilling of TiAl6V4. *Journal of Materials Processing Technology*, 2018, 262: 131–148.
[109] H J Yang, W F Ding, Y Chen, et al. Drilling force model for forced low frequency vibration assisted drilling of Ti-6Al-4V titanium alloy. *International Journal of Machine Tools and Manufacture*, 2019,146: 103438.
[110] H J Yang, Y Chen, J H Xu, et al. Chip control analysis in low-frequency vibration-assisted drilling of Ti–6Al–4V titanium alloys. *International Journal of Precision Engineering and Manufacturing*, 2020, 21(4): 565–584.
[111] Z J Zhu, K Guo, J Sun, et al. Evolution of 3D chip morphology and phase transformation in dry drilling Ti6Al4V alloys. *Journal of Manufacturing Processes*, 2018, 34: 531–539.
[112] K Okamura, H Sasahara, T Segawa, et al. Low-frequency vibration drilling of titanium alloy. *JSME International Journal Series C Mechanical Systems, Machine Elements and Manufacturing*, 2006, 49(1): 76–82.
[113] K Okamura, H Sasahara. Prediction of drilling temperature during low-frequency vibration drilling of titanium alloy. *Journal of Advanced Mechanical Design, Systems, and Manufacturing*, 2017, 11(3): JAMDSM0036.
[114] O Pecat, E Brinksmeier. Tool wear analyses in low frequency vibration assisted drilling of CFRP/Ti6Al4V Stack material. *Procedia CIRP*, 2014, 14: 142–147.
[115] O Pecat, E Brinksmeier. Low damage drilling of CFRP/Titanium compound materials for fastening. *Procedia CIRP*, 2014,13: 1–7.
[116] R Hussein, A Sadek, M A Elbestawi, et al. Low-frequency vibration-assisted drilling of hybrid CFRP/Ti6Al4V stacked material. *The International Journal of Advanced Manufacturing Technology*, 2018, 98(9): 2801–2817.
[117] Q W Yao, Y Chen, H J Yang. et al. Influence of amplitude on low frequency vibration drilling CFRP/titanium alloy stack materials. *Aeronautical Manufacturing Technology*, 2018, 61(6): 64–69. (in Chinese)
[118] A Sadek, M H Attia, M Meshreki, et al. Characterization and optimization of vibration-assisted drilling of fibre reinforced epoxy laminates. *CIRP Annals - Manufacturing Technology*, 2013, 62(1): 91–94.
[119] Z Li, D Y Zhang, X G Jiang, et al. Study on rotary ultrasonic-assisted drilling of titanium alloys (Ti6Al4V) using 8-facet drill under no cooling condition. *The International Journal of Advanced Manufacturing Technology*, 2017, 90(9): 3249–3264.

[120] Y S Liao, Y C Chen, H M Lin. Feasibility study of the ultrasonic vibration assisted drilling of Inconel superalloy. *International Journal of Machine Tools and Manufacture*, 2007, 47(12–13): 1988–1996.

[121] Z Y Shao, X G Jiang, Z Li, et al. Feasibility study on ultrasonic-assisted drilling of CFRP/Ti stacks by single-shot under dry condition. *The International Journal of Advanced Manufacturing Technology*, 2019, 105(1): 1259–1273.

[122] Z Y Shao, X G Jiang, D X Geng, et al. The interface temperature and its influence on surface integrity in ultrasonic-assisted drilling of CFRP/Ti stacks. *Composite Structures*, 2021, 266: 113803.

[123] A Sanda, I Arriola, V G Navas, et al. Ultrasonically assisted drilling of carbon fibre reinforced plastics and Ti6Al4V. *Journal of Manufacturing Processes*, 2016, 22: 169–176.

[124] D X Geng, Z H Lu, G Yao, et al. Cutting temperature and resulting influence on machining performance in rotary ultrasonic elliptical machining of thick CFRP. *International Journal of Machine Tools and Manufacture*, 2017, 123: 163–170.

[125] Y X Li, F Jiao, S J Zhang, et al. Experimental study on high and low frequency compound vibration-assisted drilling of CFRP / titanium alloy laminated structure. *Acta Aeronautica et Astronautica Sinica*, 2021, 42(10): 344–357. (in Chinese)

[126] W L Cong, X T Zou, T W Deines, et al. Rotary ultrasonic machining of carbon fiber reinforced plastic composites: An experimental study on cutting temperature. *Journal of Reinforced Plastics and Composites*, 2012, 31(22): 1516–1525.

[127] F Makhdum, V A Phadnis, A Roy, et al. Effect of ultrasonically-assisted drilling on carbon-fibre-reinforced plastics. *Journal of Sound and Vibration*, 2014, 333(23): 5939–5952.

[128] M P Yan, H Shao. Analysis of temperature and wear of tool of ultrasonic vibration drilling Ti alloys. *Tool Engineering*, 2011, 45(8): 26–30. (in Chinese)

[129] J Pujana, A Rivero, A Celaya, et al. Analysis of ultrasonic-assisted drilling of Ti6Al4V. *International Journal of Machine Tools and Manufacture*, 2008, 49(6): 500–508.

[130] M A Moghaddas, A Y Yi, K F Graff. Temperature measurement in the ultrasonic-assisted drilling process. *The International Journal of Advanced Manufacturing Technology*, 2019, 103(1–4): 187–199.

[131] B Denkena, D Boehnke, J H Dege. Helical milling of CFRP–titanium layer compounds. *CIRP Journal of manufacturing Science and Technology*, 2008, 1(2): 64–69.

[132] B Denkena, D Nespor, M Rehe, et al. Process force prediction in orbital drilling of process force prediction in orbital drilling of TiAl6V4. *Proceedings of the 9th International Conference on Advanced Manufacturing Systems and Technology*, 2011: 113–128.

[133] G L Yang, Z G Dong, R K Kang, et al. Research progress of helical milling technology. *Acta Aeronautica et Astronautica Sinica*, 2020, 41(7): 18–32. (in Chinese)

[134] E Brinksmeier, S Fangmann, R Rentsch. Drilling of composites and resulting surface integrity. *CIRP Annals - Manufacturing Technology*, 2011, 60(1): 57–60.

[135] B Wang, Y F Wang, H Zhao, et al. Effect of a Ti alloy layer on CFRP hole quality during helical milling of CFRP/Ti laminate. *Composite Structures*, 2020, 252: 112670.

[136] A Barman, R Adhikari, G Bolar. Evaluation of conventional drilling and helical milling for processing of holes in titanium alloy Ti6Al4V. *Materials Today: Proceedings*, 2020, 28: 2295–2300.

[137] A Sadek, M Meshreki, M H Attia. Characterization and optimization of orbital drilling of woven carbon fiber reinforced epoxy laminates. *CIRP Annals - Manufacturing Technology*, 2012, 61(1): 123–126.

[138] J L Cantero, M M Tardío, J A Canteli, et al. Dry drilling of alloy Ti–6Al–4V. *International Journal of Machine Tools and Manufacture*, 2005, 45(11): 1246–1255.

[139] S Sakamoto, H Iwasa. Effect of cutting revolution speed on cutting temperature in helical milling of cfrp composite laminates. *Key Engineering Materials*, 2012, 523: 58–63.

[140] J Liu. *Study on cutting heat and temperature prediction in helical milling for CFRP/titanium*. Tianjin: Tianjin University, 2014. (in Chinese)

[141] J Liu, G Chen, C H Ji, et al. An investigation of workpiece temperature variation of helical milling for carbon fiber reinforced plastics (CFRP). *International Journal of Machine Tools and Manufacture*, 2014, 86: 89–103.

[142] J Liu, C Z Ren, X D Qin, et al. Prediction of heat transfer process in helical milling. *The International Journal of Advanced Manufacturing Technology*, 2014, 72(5–8): 693–705.

[143] S C Tam, C Y Yeo, S Jana, et al. Optimization of laser deep-hole drilling of Inconel 718 using the Taguchi method. *Journal of Materials Processing Technology*, 1993, 37(1–4): 741–757.

[144] S Sharma, V Mandal, S A Ramakrishna, et al. Numerical simulation of melt hydrodynamics induced hole blockage in Quasi-CW fiber laser micro-drilling of TiAl6V4. *Journal of Materials Processing Technology*, 2018, 262: 131–148.

[145] A Bharatish, H N N Murthy, B Anand, et al. Characterization of hole circularity and heat affected zone in pulsed CO2 laser drilling of alumina ceramics. *Optics and Laser Technology*, 2013, 53: 22–32.

[146] A Luft, U Franz, L Emsermann, et al. A study of thermal and mechanical effects on materials induced by pulsed laser drilling. *Applied Physics A*, 1996, 63(2): 93–101.

[147] S Bandyopadhyay, J K Sarin Sundar, G Sundararajan, et al. Geometrical features and metallurgical characteristics of Nd: YAG laser drilled holes in thick IN718 and Ti–6Al–4V sheets. *Journal of Materials Processing Technology*, 2002, 127(1): 83–95.

[148] A Y Mustafa. Modelling of the hole quality characteristics by extreme learning machine in fiber laser drilling of Ti-6Al-4V. *Journal of Manufacturing Processes*, 2018, 36: 138–148.

[149] S Chatterjee, S S Mahapatra, A Mondal, et al. An experimental study on drilling of titanium alloy using CO2 laser. *Sādhanā*, 2018, 43(8): 1–14.

[150] S Mishra, V Yadava. Modeling and optimization of laser beam percussion drilling of thin aluminum sheet. *Optics and Laser Technology*, 2013, 48: 461–474.

[151] S Mishra, V Yadava. Modelling of hole taper and heat affected zone due to laser beam percussion drilling. *Machining Science and Technology*, 2013, 17(2): 270–291.

[152] C Leone, S Genna. Heat affected zone extension in pulsed Nd: YAG laser cutting of CFRP. *Composites Part B: Engineering*, 2018, 140: 174–182.

[153] R Weber, M Hafner, A Michalowski, et al. Minimum damage in CFRP laser processing. *Physics Procedia*, 2011, 12: 302–307.

[154] Y Y Ye, S H Jia, Z F Xu, et al. Research on hole drilling in carbon fiber reinforced composite by using laser cutting method. *Aeronautical Manufacturing Technology*, 2019, 62(18): 50–55. (in Chinese)

[155] W Y Li, Y Huang, X H Chen, et al. Study on laser drilling induced defects of CFRP plates with different scanning modes based on multi-pass strategy. *Optics and Laser Technology*, 2021, 144: 107400.

[156] D Y Pimenov, M Mia, M K Gupta, et al. Improvement of machinability of Ti and its alloys using cooling-lubrication techniques: a review and future prospect. *Journal of Materials Research and Technology*, 2021, 11: 719–753.

[157] S Deshpande, Y Deshpande. A review on cooling systems used in machining processes. *Materials Today: Proceedings*, 2019, 18: 5019–5031.

[158] A E I Elshwain, N Redzuan. Effect of cooling/lubrication using cooled air, MQL + cooled Air, N_2 and CO_2 gases on tool life and surface finish in machining – A review. *Advanced Materials Research*, 2014, 845: 889–893.

[159] E M Rubio, B Agustina, M Marín, et al. Cooling systems based on cold compressed air: A review of the applications in machining processes. *Procedia Engineering*, 2015, 132: 413–418.

[160] M Cuesta, P Aristimuño, A Garay, et al. Heat transferred to the workpiece based on temperature measurements by IR technique in dry and lubricated drilling of Inconel 718. *Applied Thermal Engineering*, 2016, 104: 309–318.

[161] K Park, J Olortegui-Yume, M Yoon, et al. A study on droplets and their distribution for minimum quantity lubrication (MQL). *International Journal of Machine Tools and Manufacture*, 2010, 50(9): 824–833.

[162] B Boswell, M N Islam, I J Davies, et al. A review identifying the effectiveness of minimum quantity lubrication (MQL) during conventional machining. *The International Journal of Advanced Manufacturing Technology*, 2017, 92(1): 321–340.

[163] V S Sharma, G Singh, K Sørby. A review on minimum quantity lubrication for machining processes. *Materials and Manufacturing Processes*, 2015, 30(8): 935–953.

[164] N N N Hamran, J A Ghani, R Ramli, et al. A review on recent development of minimum quantity lubrication for sustainable machining. *Journal of Cleaner Production*, 2020, 268: 122165.

[165] N T Mathew, L Vijayaraghavan. Environmentally friendly drilling of intermetallic titanium aluminide at different aspect ratio. *Journal of Cleaner Production*, 2017, 141: 439–452.
[166] J Y Xu, M Ji, J P Davim, et al. Comparative study of minimum quantity lubrication and dry drilling of CFRP/titanium stacks using TiAlN and diamond coated drills. *Composite Structures*, 2020, 234: 111727.
[167] J Y Xu, M Ji, M Chen, et al. Investigation of minimum quantity lubrication effects in drilling CFRP/Ti6Al4V stacks. *Materials and Manufacturing Processes*, 2019, 34(12): 1401–1410.
[168] S Bhowmick, A T Alpas. Minimum quantity lubrication drilling of aluminium–silicon alloys in water using diamond-like carbon coated drills. *International Journal of Machine Tools and Manufacture*, 2008, 48(12–13): 1429–1443.
[169] E A Rahim, H Sasahara. High speed MQL drilling of titanium alloy using synthetic ester and palm oil. *Proceedings of the 36th International MATADOR Conference*, Springer London, 2010: 193–196.
[170] N T Mathew, V Laxmanan. Temperature rise in workpiece and cutting tool during drilling of titanium aluminide under sustainable environment. *Materials and Manufacturing Processes*, 2018, 33(16): 1765–1774.
[171] K S Murthy, I G Rajendran. Prediction and analysis of multiple quality characteristics in drilling under minimum quantity lubrication. *Proceedings of the Institution of Mechanical Engineers, Part B: Journal of Engineering Manufacture*, 2012, 226(6): 1061–1070.
[172] J F Kelly, M G Cotterell. Minimal lubrication machining of aluminium alloys. *Journal of Materials Processing Technology*, 2002, 120(1): 327–334.
[173] R P Zeilmann, W L Weingaertner. Analysis of temperature during drilling of Ti6Al4V with minimal quantity of lubricant. *Journal of Materials Processing Technology*, 2006, 179(1): 124–127.
[174] E Brinksmeier, R Janssen. Drilling of multi-layer composite materials consisting of carbon fiber reinforced plastics (CFRP), titanium and aluminum alloys. *CIRP Annals - Manufacturing Technology*,2002, 51(1): 87–90.
[175] U S Dixit, D K Sarma, J P Davim. *Environmentally friendly machining*. Springer Science & Business Media, 2012.
[176] Y Su, N He, L Li, et al. Refrigerated cooling air cutting of difficult-to-cut materials. *International Journal of Machine Tools and Manufacture*, 2006, 47(6): 927–933.
[177] S J Ha, K B Kim, J K Yang, et al. Influence of cutting temperature on carbon fiber-reinforced plastic composites in high-speed machining. *Journal of Mechanical Science and Technology*, 2017, 31(4): 1861–1867.
[178] S Sun, M Brandt, M S Dargusch. Machining Ti–6Al–4V alloy with cryogenic compressed air cooling. *International Journal of Machine Tools and Manufacture*, 2010, 50(11): 933–942.
[179] C Li, J Xu, M Chen, et al. Tool wear processes in low frequency vibration assisted drilling of CFRP/Ti6Al4V stacks with forced air-cooling. *Wear*, 2019, 426: 1616–1623.
[180] M Rahman, A S Kumar, M U Salam, et al. Effect of chilled air on machining performance in end milling. *International Journal of Advanced Manufacturing Technology*, 2003, 21(10): 787–795.
[181] M K N Khairusshima, C H C Hassan, A G Jaharah, et al. Effect of chilled air on tool wear and workpiece quality during milling of carbon fibre-reinforced plastic. *Wear*, 2013, 302(1–2): 1113–1123.
[182] P Asok, P Chockalingam. Dry and compressed air cooling comparative study on 6061 aluminium alloy drilling using coated drill. *Advanced Materials Research*, 2014, 903: 45–50.
[183] B Tasdelen, T Wikblom, S Ekered. Studies on minimum quantity lubrication (MQL) and air cooling at drilling. *Journal of Materials Processing Technology*, 2007, 200(1): 339–346.
[184] R Domingo, B de Agustina, M M Marín. Study of drilling process by cooling compressed air in reinforced polyether-ether-ketone. *Materials*, 2020, 13(8): 1965.
[185] J Liu, Y K Chou. On temperatures and tool wear in machining hypereutectic Al–Si alloys with vortex-tube cooling. *International Journal of Machine Tools and Manufacture*, 2007, 47: 635–645.
[186] W W Wu, A T Kuzu, D Stephenson, et al. Dry and minimum quantity lubrication high-throughput drilling of compacted graphite iron. *Machining Science and Technology*, 2018, 22(4): 652–670.
[187] A Kuzu, W W Wu, D Stephenson, et al. High-throughput dry and minimum quantity lubrication drilling of compacted graphite iron. *Procedia CIRP*, 2016, 46: 87–90.
[188] J S Nam, P Lee, S W Lee. Experimental characterization of micro-drilling process using nanofluid minimum quantity lubrication. *International Journal of Machine Tools and Manufacture*, 2011, 51(7–8): 649–652.
[189] F J Wang, D Cheng, B Y Zhang, et al. Reversed-air cooling technology for high-quality drilling of CFRP. *Applied Composite Materials*, 2019, 26(3): 857–870.
[190] R Fu, Z Y Jia, F J Wang, et al. Cooling process of reverse air suctioning for damage suppression in drilling CFRP composites. *Procedia CIRP*, 2019, 85: 147–152.
[191] S Cordes, F Hübner, T Schaarschmidt. Next generation high performance cutting by use of carbon dioxide as cryogenics. *Procedia CIRP*, 2014, 14: 401–405.
[192] K Park, M A Suhaimi, G D Yang, et al. Milling of titanium alloy with cryogenic cooling and minimum quantity lubrication (MQL). *International Journal of Precision Engineering and Manufacturing*, 2017, 18(1): 5–14.
[193] O Pereira, H González, A Calleja, et al. Manufacturing of human knee by cryogenic machining: Walking towards cleaner processes. *Procedia Manufacturing*, 2019, 41: 257–263.
[194] W Zhao, F Ren, A Iqbal, et al. Effect of liquid nitrogen cooling on surface integrity in cryogenic milling of Ti-6Al-4 V titanium alloy. *The International Journal of Advanced Manufacturing Technology*, 2020, 106(2): 1497–1508.
[195] M I Sadik, S Isakson, A Malakizadi, et al. Influence of coolant flow rate on tool life and wear development in cryogenic and wet milling of Ti-6Al-4V. *Procedia CIRP*, 2016, 46: 91–94.
[196] S Y Hong, I Markus, W C Jeong. New cooling approach and tool life improvement in cryogenic machining of titanium alloy Ti-6Al-4V. *International Journal of Machine Tools and Manufacture*, 2001, 41(15): 2245–2260.
[197] U Kumar, P Senthil. A comparative machinability study on titanium alloy Ti-6Al-4V during dry turning by cryogenic treated and untreated condition of uncoated WC inserts. *Materials Today: Proceedings*, 2020, 27: 2324–2328.
[198] A Rodríguez, A Calleja, L N L de López, et al. Drilling of CFRP-Ti6Al4V stacks using CO_2-cryogenic cooling. *Journal of Manufacturing Processes*, 2021, 64: 58–66.
[199] P Shah, N Khanna, A K Singla, et al. Tool wear, hole quality, power consumption and chip morphology analysis for drilling Ti-6Al-4V using LN2 and LCO2. *Tribology International*, 2021, 163: 107190.
[200] K Navneet, S Prassan, W Jwalant, et al. Energy consumption and lifecycle assessment comparison of cutting fluids for drilling titanium alloy. *Procedia CIRP*, 2021, 98: 175–180.
[201] M P Kumar, L S Ahmed. Drilling of AISI 304 stainless steel under liquid nitrogen cooling: A comparison with flood cooling. *Materials Today: Proceedings*, 2017, 4(2): 1518–1524.
[202] I S Jawahir, H Attia, D Biermann, et al. Cryogenic manufacturing processes. *CIRP Annals - Manufacturing Technology*, 2016, 65(2): 713–736.
[203] M Perçin, K Aslantas, İ Ucun, et al. Micro-drilling of Ti–6Al–4V alloy: The effects of cooling/lubricating. *Precision Engineering*, 2016, 45: 450–462.
[204] L S Ahmed, M P Kumar. Multiresponse optimization of cryogenic drilling on Ti-6Al-4V alloy using topsis method. *Journal of Mechanical Science and Technology*, 2016, 30(4): 1835–1841.
[205] L S Ahmed, M P Kumar. Cryogenic drilling of Ti–6Al–4V alloy under liquid nitrogen cooling. *Materials and Manufacturing Processes*, 2016, 31(7): 951–959.
[206] S Barnes, P Bhudwannachai, A Dahnel. Drilling performance of carbon fiber reinforced epoxy composite when machined dry, with conventional cutting fluid and with a cryogenically cooled tool. *ASME International Mechanical Engineering Congress and Exposition. American Society of Mechanical Engineers*, 2013, 56192: V02BT02A063.
[207] N Uçak, A Çiçek. The effects of cutting conditions on cutting temperature and hole quality in drilling of Inconel 718 using solid carbide drills. *Journal of Manufacturing Processes*, 2018, 31: 662–673.
[208] N W Sorbo, J J Dionne. Dry drilling of stackup composite: Benefits of CO_2 cooling. *SAE International Journal of Aerospace*, 2014, 7(1): 156.
[209] M I Sadik, G Grenmyr. Application of different cooling strategies in drilling of metal matrix composite (MMC). *Materials Science Forum*, 2016, 836: 3–12.